國 立 交 通 大 學

電信工程研究所

碩 士 論 文

上行多點協調式系統之傳收機設計

Transceiver Design for Uplink Coordinated Multipoint Systems

研 究 生：梁曉婷　　Student: Hsiao-Ting Liang

指導教授：李大嵩 博士　　Advisor: Dr. Ta-Sung Lee

中 華 民 國 一 百 零 一 年 九 月

上行多點協調式系統之傳收機設計

Transceiver Design for Uplink Coordinated Multipoint Systems

研 究 生：梁曉婷　　Student: Hsiao-Ting Liang

指導教授：李大嵩博士　　Advisor: Dr. Ta-Sung Lee

國立交通大學

電信工程研究所

碩士論文

A Thesis
Submitted to Institute of Communications Engineering
College of Electrical and Computer Engineering
National Chiao Tung University
in Partial Fulfillment of the Requirements
for the Degree of
Master of Science
in
Communications Engineering

September 2012

Hsinchu, Taiwan, Republic of China

中 華 民 國 一 百 零 一 年 九 月

上行多點協調式系統之傳收機設計

學生：梁曉婷　　指導教授：李大嵩　博士

國立交通大學電信工程研究所碩士班

摘要

為了達到下世代蜂巢式無線系統更進一步的性能要求，多種典型的技術在這種受限於干擾的環境下被發展出來。多點協調(coordinated multipoint; CoMP)傳輸與接收技術以及多輸入多輸出(multiple input multiple output; MIMO)技術為其中兩種對抗干擾之關鍵性技術。在本篇論文中，吾人於集中式上行傳輸多點協調系統中提出兩種多天線、多資料串流之疊代式傳收機設計。第一種傳收機設計引入干擾校齊(interference alignment; IA)的概念，可達到干擾校齊以及干擾抑制的作用。第二種傳收機設計則是藉由最小化有效通道矩陣之條件數以及最大化有效通道矩陣之奇異值以強化有效通道之條件。根據模擬結果，吾人所提出之方法具有優秀的收斂特性。再者，在少數疊代運算內就可達到較好的速率總和、較為公平的結果，並且對於疊代運算中的初始值較為穩定。

Transceiver Design for Uplink Coordinated Multipoint Systems

Student: Hsiao-Ting Liang Advisor: Dr. Ta-Sung Lee

Institute of Communications Engineering

National Chiao Tung University

Abstract

To achieve advanced performance requirements for the next generation cellular wireless systems, several classic techniques have been developed under such interference limited environments. Coordinated multipoint (CoMP) transmission and reception and multiple input multiple output (MIMO) systems are two key techniques to overcome the effect caused by interference. In this thesis, two iterative centralized uplink CoMP transceiver schemes are proposed where multiple antennas and multiple transmit layers are assumed. The fist one incorporates the idea of a new emerging technique, interference alignment (IA) which can align and then mitigate the interference. The second proposed method is developed to enhance the effective channel condition by minimizing the condition number and maximizing the singular values of the effective channel matrix. According to the simulation results, the proposed methods can provide superior convergence behavior. The results also show that they achieve rather good sum-rate performance, provide robustness to the initial values in the iterative procedures, and lead to much fairer results, within few iterations.

Acknowledgement

First, I would like to express my sincere gratitude to my advisor, Dr. Ta-Sung Lee, for his guidance and inspiring discussions. His positive and conscientious attitude in research has benefited me in my study as well. Also, I am really grateful to all my friends and the members in the Communication System Design and Signal Processing (CSDSP) Lab for their constant encouragement and help. Finally, I would like to thank my family for their tremendous love, kind words, and support.

Table of Contents

List of Figures

List of Tables

Acronym Glossary

3GPP	third generation partnership project
BC	broadcast channel
BS	base station
CoMP	coordinated multipoint
CSI	channel state information
CU	central unit
DL	downlink
DoF	degrees of freedom
IA	interference alignment
ICI	inter cell interference
LTE-A	long term evolution-advanced
MAC	multiple access channel
MIMO	multiple input multiple output
MMSE	minimum mean square error
RRH	remote radio head
SINR	signal to interference and noise ratio
SNR	signal to noise ratio
UE	user equipment
UL	uplink

Notations

K	number of cells in the cooperation group
u	number of UEs in each cell
M_t	number of transmit antennas
M_r	number of receive antennas
$\mathbf{s}_k^i$	transmitted signal vector of the *i*th UE in the *k*th cell
$\mathbf{V}_k^i$	precoder matrix of the *i*th UE in the *k*th cell
$\mathbf{H}_{k,l}^i$	channel between the *k*th BS and the *i*th UE in cell *l*
$\mathbf{V}$	collective precoder matrix
$\mathbf{U}$	decoder matrix
$\mathbf{H}$	collective channel matrix
$\mathbf{F}$	receiver matrix
d_T	number of total transmit data streams
$\mathbf{I}_M$	identity matrix of size $M \times M$
$\mathrm{diag}\{\cdot\}$	block diagonal matrix staking operator
$\mathbf{X}^T$	transpose operator
$\mathbf{X}^H$	Hermitian operator
$\mathbf{X}^{-1}$	inverse operation
$\mathrm{E}\{\cdot\}$	expectation operator
$\mathrm{tr}(\cdot)$	trace operator
$\det(\cdot)$	determinant operator
$[\mathbf{x}^H]_{(i)}$	*i*th element of row vector $\mathbf{x}^H$
$\mathbf{X}^{(i)}$	the *i*th column of matrix $\mathbf{X}$
$\{\mathbf{X}\}_i^j$	matrix consists of the *i*th column to *j*th column of matrix $\mathbf{X}$
$[\mathbf{X}]_{i,i}$	*i*th diagonal element

Chapter 1

Introduction

The increasing demand for wireless equipments stimulates the evolution of existing mobile wireless communication systems to achieve higher data rates and more reliable link quality. Furthermore, due to the concern for scarcity of spectrum, unity frequency reuse is adopted in the next generation wireless communication system which would cause severe inter-cell interference (ICI). To meet performance requirements under such strict environments, advanced techniques have been developed such as coordinated multipoint (CoMP) transmission and reception and multiple input multiple output (MIMO) systems. These two techniques are provided as key solutions to alleviate the impact caused by ICI in the 4G mobile cellular standards, e.g. 3GPP LTE-Advanced [1].

CoMP is a technique that utilizes the cooperation between points in some cooperation group to coordinate the transmission/reception which is controlled by a central unit (CU) for the purpose of ICI alleviation and quality enhancement. CoMP has been adopted in practical cellular systems as a tool to improve cell coverage and cell edge throughput. In practice, CoMP can be classified by the capability of backhauling into full cooperation CoMP and partial cooperation CoMP [2]-[3]. Exchange of full information including full channel state information (CSI) and full data information is

allowed in full cooperation CoMP with less backhaul constraints. Centralized CoMP which can provide joint transmission or reception is one of the examples [4]-[5]. On the other hand, partial cooperation exchanges partial data and CSI. For this type of CoMP, distributed CoMP and coordinated scheduling are two typical approaches [2], [5].

MIMO exploits the spatial degrees of freedom provided by multiple antennas to offer improved system capacity and/or diversity for better link quality. It has become a promising technique in most existing communication standards. A great deal of research works have been done on the applications of MIMO in cellular systems. Using MIMO in a multi-user system inevitably increases the interference level for each user, so there is a need to develop methods for mitigating the inter-user interference [6].

Due to the potential for system performance improvement, centralized CoMP is considered as our research platform, where the CU jointly processes the received signals from all the BSs with full information exchange. Based on this structure, there is a common assumption that user equipment (UE) is equipped with a single antenna owing to cost, hardware, and size constraints. Thanks to the evolution of technology, multiple antennas are now available at UE in practical cellular network. Hence, centralized CoMP with multiple transmit and multiple receive antennas (MIMO) has attracted a lot of attention, and there are abundant researches that focus on the problem with a single transmit data stream (single transmit layer) [7]. However, the case with multiple transmit layers in centralized CoMP has not been widely studied. Therefore, to further improve communication efficiency, two transceiver schemes in centralized CoMP with multiple antennas and multiple transmit layers are developed in this thesis, and the study is focus on the uplink case due to no resource-consuming CSI feedback is needed.

Each of our two proposed algorithms includes precoders, a joint decoder, and a linear MMSE receiver, and is iterative in nature. In each iteration, two stage calculations are involved: 1) to calculate the joint decoder based on given precoders and 2) to compute the precoders based on a given decoder. The fist proposed transceiver scheme, called "IA aided UL CoMP", incorporates the idea of a new emerging technique, interference alignment (IA). IA has recently developed for the X-channel and K-user interference channel as a capacity approaching technique [8]-[9]. The basic idea of IA is to align or compress interference into some limited subspace so the interference can be separated from the desired signal with sufficient degrees of freedom (DoF). The second proposed transceiver scheme, called "Channel condition enhanced UL CoMP", is developed to enhance the effective channel condition by minimizing the condition number and maximizing the singular values of the effective channel matrix. UL-DL duality is also exploited in the second proposed method. All the simulation results show that both of the proposed approaches achieve superior system performance.

The thesis is organized as follows. The mathematical system model of centralized UL CoMP, the definition of achievable sum-rate, and the introduction of IA in *K*-user interference channel are illustrated in Chapter 2. In Chapter 3, the basic idea and the derivation of the proposed IA aided UL CoMP are illustrated. The proposed Channel condition enhanced UL CoMP is developed in Chapter 4. In the same chapter, complexity analysis and numerical evaluations of the two proposed methods are also provided. Finally, summary of our works and several potential future works are given in Chapter 5.

Chapter 2

System Model

The exponential growth of mobile data traffic and the demands of better link quality trigger the evolution of existing mobile wireless communication systems. To achieve the higher requirement of spectrum efficiency in next generation wireless systems, e.g., 3GPP LTE-Advanced, some typical communication schemes are adopted such as unity frequency reuses and multiuser transmission scheme, and that leads to an interference limited environment. Coordinated multipoint (CoMP) transmission and reception and multiple input multiple output (MIMO) systems are two key techniques proposed to overcome the effect caused by interference. In this thesis, we consider uplink CoMP (UL CoMP) assisted with multiple antennas as our system model, and two associated transceiver schemes are proposed, among which one incorporates the idea of interference alignment (IA), a recently emerged interference mitigation criterion.

In section 2.1, the classification of CoMP systems will be presented, and then we address the UL CoMP scheme adopted in this thesis. According to the considered UL CoMP scheme, the mathematical system model of multicell multiuser MIMO system and the transceiver design are introduced in section 2.2. Besides, we describe the performance metrics in terms of achievable sum-rate employing linear MMSE receiver.

Interference alignment has recently emerged as a generalized multi-user MIMO technique for the X-channel and *K*-user interference channel scenarios. Its superior performance of interference mitigation has been proven, and it will be incorporated into one of our transceiver design. The basic idea of IA in *K*-user interference channel is presented in section 2.3.

2.1 Uplink Coordinated Multipoint (CoMP) System Model

In modern cellular communication systems, user equipment (UE) in the cell-edge region can sustain superior interference which will cause serious degradation of link quality. To cope with the issues caused by interference and further improve the system efficiency, coordinated multipoint (CoMP) transmission and reception are developed. The main idea is to utilize the cooperation between points (BSs or RRHs) in some cooperation group to operate joint transmission/reception and interference mitigation/avoidance, so better cell coverage and cell edge throughput could thus be achieved. The benefits provided by CoMP have been evaluated, and CoMP is adopted in some cellular networks, e.g., LTE-Advanced as a key technique. In practice, the cooperation in CoMP is restricted due to restricted latency and limited backhauling, and this leads to different CoMP schemes, with either full cooperation or partial cooperation [2]-[3]. In this thesis, a centralized UL CoMP with full cooperation is considered.

CoMP with full cooperation exchanges information including full channel side information (CSI) and full data information. Centralized CoMP with joint transmission /reception is a typical full cooperation approach which is controlled by a central unit (CU) that could be any point in the cooperation set as depicted in **Figure 2-1** [4]-[5]; it is applicable to scenarios with less backhaul constraints such as that provided in

LTE-Advanced standard. In LTE-Advanced, scenario 1 is the homogeneous network aiming for intrasite multipoint coordination where no backhaul connection is needed, as illustrated in **Figure 2-2**. Scenario 2/3/4 is the homogeneous network with remote radio heads (RRHs) where the connection between coordinated points is provided by optical fiber which supports small latency and ample bandwidth, as illustrated in **Figure 2-3** and **Figure 2-4** [1], [5]. On the other hand, partial cooperation exchanges partial data and CSI. Distributed CoMP and coordinated scheduling are two approaches of partial cooperation [2], [5]. According to the potential for system performance improvement, we focus on centralized UL CoMP in this thesis.

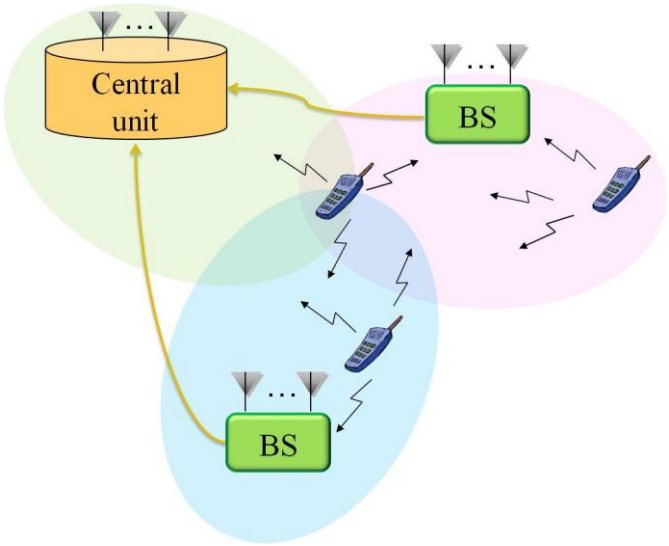

Figure 2-1: Centralized CoMP scheme controlled by a central unit (CU)

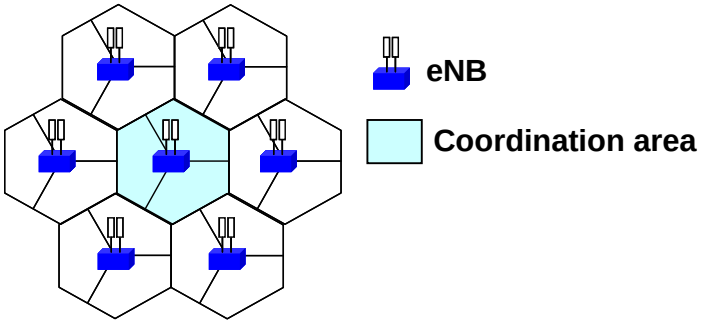

Figure 2-2: Scenario 1 (homogeneous network with intra-site CoMP)[1]

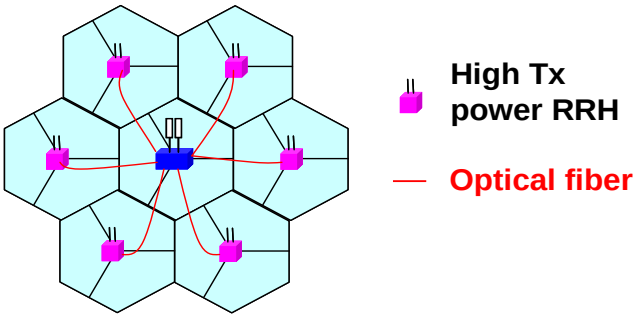

Figure 2-3: Scenario 2 (homogeneous network with high Tx power RRHs)[1]

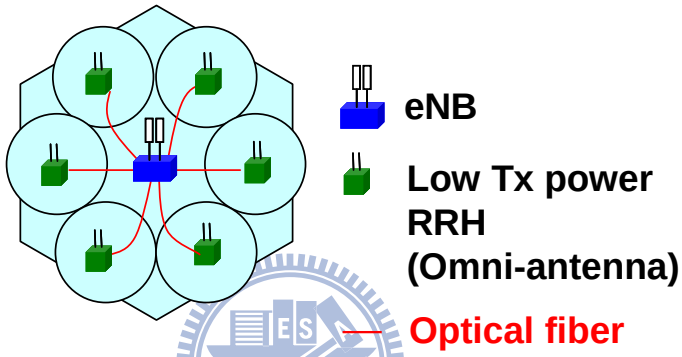

Figure 2-4: Scenario 3/4 (heterogeneous network with low power RRHs within the macrocell coverage where the RRHs have different/the same cell IDs as the macro cell)[1]

Centralized UL CoMP is a scheme that the transmitted signal from a particular user is received by multiple points in the cooperation set, and then due to full cooperation, the received signal from multiple points are joint processed at CU as illustrated in **Figure 2-5**. For the purpose of reasonable implementation complexity, linear processing is considered in this thesis. Due to the acceptable complexity and comparatively better tolerance to noise, linear MMSE receiver is adopted. In our work, multiple antennas are at both transmit and receive sides, and multiple transmit layers is assumed. We consider the structure that the transmitted signal vector of each UE is processed by its own linear precoder before transmission, and then with full BS

cooperation, the CU joint processes the received signal from all the BSs by linear decoder and linear MMSE receiver, successively.

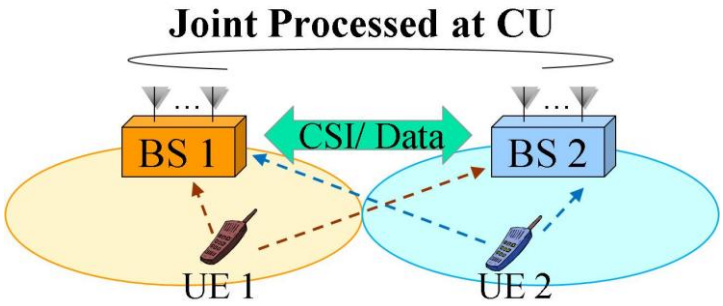

Figure 2-5: Centralized UL CoMP with full cooperation

2.2 Transceiver Structure and Associated Achievable Sum-Rate in UL CoMP

In this section, the mathematical system model of centralized UL CoMP involving multicell multiuser MIMO infrastructure is introduced; the basic structure of the associated transceiver design in this thesis is also presented in detail. Sum-rate performance is a major performance index in CoMP systems; the achievable sum-rate of centralized UL CoMP system equipped with linear MMSE receiver will be demonstrated.

Based on the structure of centralized UL CoMP, a typical minimum sum mean square error (MMSE) transceiver depicted in **Figure 2-6** has been proposed in [10]. The precoders $\mathbf{V}_i^j$ and the linear MMSE receiver **F** are calculated iteratively based on MMSE criterion. However, it exhibits a poor convergence behavior as illustrated in **Figure 2-7**, where the number of transmit layers, transmit antennas, and receive antennas are 2, 4, and 2, respectively. For more efficient communication schemes, two transceiver designs are proposed in this thesis. Based on the property of the MMSE

receiver, a well-conditioned effective channel (consists of $\mathbf{V}_i^j$ and **F**) is formed when the iterative process converges. According to this property, we introduce a joint decoder **U** at CU that provides additional dimensions to facilitate the formation of a well-conditioned effective channel as depicted in **Figure 2-8**, which is equivalent to accelerating the rate of convergence.

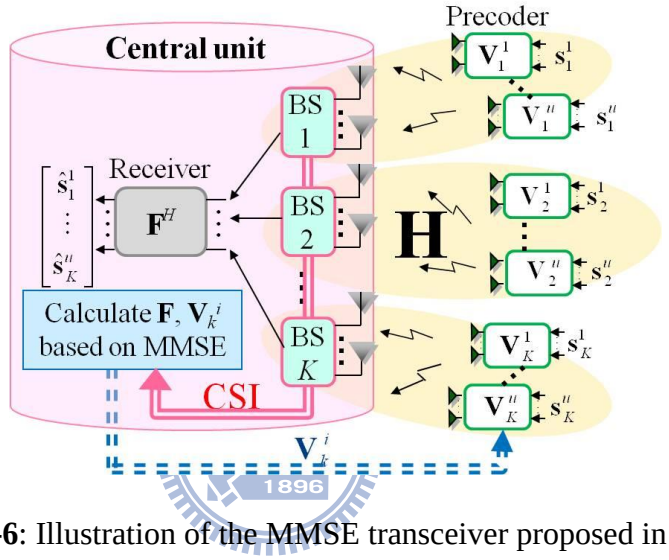

Figure 2-6: Illustration of the MMSE transceiver proposed in [10]

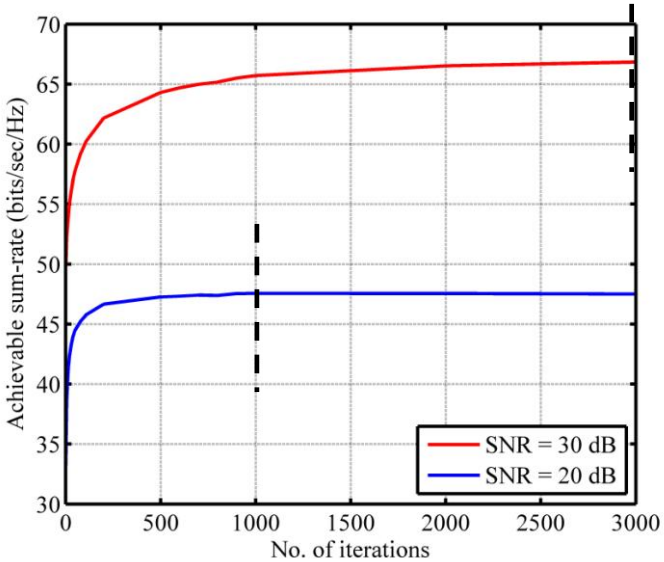

Figure 2-7: Rate convergence behavior of MMSE transceiver [10] with $K = 3$, $u = 1$

The considered uplink CoMP system involves K BSs (K cells), each equipped with M_r antennas. There are u UEs within the coverage of a BS. Each UE has M_t transmit antennas. The transmitted signal vector of the ith UE in kth cell is $\mathbf{s}_k^i \in \mathbb{C}^{d_k \times 1}$ ($\mathrm{E}\left\{\mathbf{s}_k^i \mathbf{s}_k^{i\,H}\right\} = \mathbf{I}_{d_k}$) where d_k is called the number of layers and is processed by the precoder matrix $\mathbf{V}_k^i \in \mathbb{C}^{M_t \times d_k}$ before transmission as illustrated in **Figure 2-8**. Here we denote the channel matrix between the ith UE in lth cell and the kth BS as $\mathbf{H}_{k,l}^i \in \mathbb{C}^{M_r \times M_t}$, the total transmit signal dimension of lth cell as $u \times d_l$, the total transmit signal dimension of the system as $d_T = \sum_{l=1}^{K} u \cdot d_l$, precoder matrix at lth cell as $\mathbf{V}_l$ = diag{ $\mathbf{V}_l^1, \cdots, \mathbf{V}_l^u$ } $\in \mathbb{C}^{(M_t u) \times (d_l u)}$, and the transmitted signal vector of lth cell as $\mathbf{s}_l$ = $[(\mathbf{s}_l^1)^T (\mathbf{s}_l^2)^T, \ldots, (\mathbf{s}_l^u)^T]^T \in \mathbb{C}^{(ud_l) \times 1}$. The received signal at the kth BS can be described as

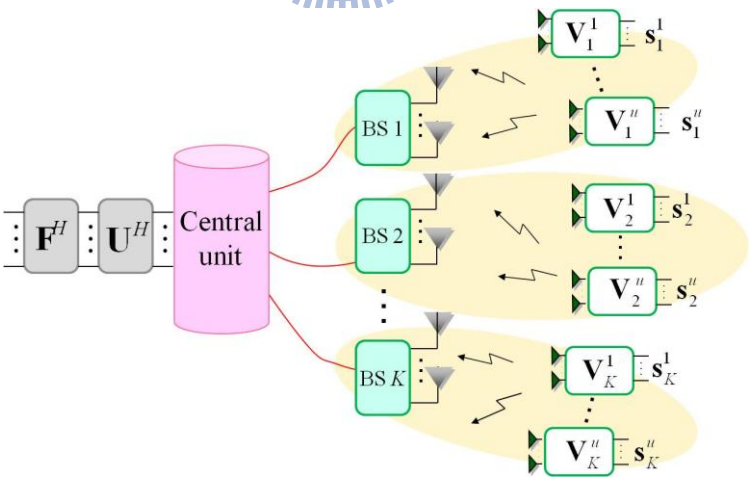

Figure 2-8: Illustration of UL CoMP sytem model

$$\mathbf{y}_k = \sum_{l=1}^{K} \mathbf{H}_{k,l} \mathbf{V}_l \mathbf{s}_l + \mathbf{n}_k, \tag{2.1}$$

where $\mathbf{H}_{k,l} \in \mathbb{C}^{M_r \times M_t u}$ is the channel matrix between the *k*th BS and all UEs in *l*th cell, and $\mathbf{n}_k \in \mathbb{C}^{M_r \times 1}$ is the noise vector with distribution $\mathrm{CN}\left(\mathbf{0}, N_0 \mathbf{I}_{M_r}\right)$. Denote the precoded signal vector as $\mathbf{x}_k^i = \mathbf{V}_k^i \mathbf{s}_k^i$. The transmit power is assumed to be restricted to *P*, i.e. $\mathrm{tr}(\mathbf{V}_k^i \mathbf{V}_k^{iH}) = P$. With full cooperation between BSs (centralized CoMP), the CU collects the received signal from all *K* BSs as follows:

$$\mathbf{y}_{\mathrm{UL\_CoMP}} = \mathbf{HVs} + \mathbf{n}, \tag{2.2}$$

where $\mathbf{H} \in \mathbb{C}^{(M_r K) \times (M_t u K)}$ is the collective channel matrix, $\mathbf{y}_{\mathrm{UL\_CoMP}} = \left[\mathbf{y}_1^T \mathbf{y}_2^T, \cdots, \mathbf{y}_K^T\right]^T \in \mathbb{C}^{(M_r K) \times 1}$, $\mathbf{V} = \mathrm{diag}\{\ \mathbf{V}_1\ , \ldots,\ \mathbf{V}_K\ \} \in \mathbb{C}^{(M_t u K) \times d_T}$, $\mathbf{s} = \left[\mathbf{s}_1^T \mathbf{s}_2^T, \cdots, \mathbf{s}_K^T\right]^T \in \mathbb{C}^{d_T \times 1}$, and $\mathbf{n} = \left[\mathbf{n}_1^T \mathbf{n}_2^T, \cdots, \mathbf{n}_K^T\right]^T \in \mathbb{C}^{(M_r K) \times 1}$. With full BS cooperation, uplink CoMP is transformed into an equivalent multiple access channel (MAC)-like system [4]. The CU processes the received signal as follows:

$$\tilde{\mathbf{y}}_{\mathrm{UL\_CoMP}} = \mathbf{U}^H \mathbf{HVs} + \mathbf{U}^H \mathbf{n} = \tilde{\mathbf{H}}\mathbf{s} + \tilde{\mathbf{n}}, \tag{2.3}$$

$$\hat{\mathbf{s}}_{\mathrm{UL\_CoMP}} = \mathbf{F}^H \tilde{\mathbf{H}}\mathbf{s} + \mathbf{F}^H \tilde{\mathbf{n}}, \tag{2.4}$$

where $\mathbf{U}^H \in \mathbb{C}^{d_T \times (M_r \times K)}$ and $\mathbf{F}^H \in \mathbb{C}^{d_T \times d_T}$ are decoder matrix and linear MMSE receiver matrix; $\hat{\mathbf{s}}$ is the estimate of $\mathbf{s}$; $\tilde{\mathbf{n}}$ is the effective noise. With precoding and decoding, the equivalent channel matrix

$$\tilde{\mathbf{H}} = \mathbf{U}^H \mathbf{HV} \tag{2.5}$$

is formed. In the rest of the paper, "Uplink CoMP" is specifically meant for the centralized UL CoMP architecture.

In this thesis, we consider closed loop UL CoMP communication system which provides better system performance while additional signaling and complexity is needed. The CU stands for the operation of precoder and decoder design based on CSI

information; hence a well-behaved augmented equivalent channel depicted at (2.5) is formed. Compared to DL case, UL CoMP closed loop communication system has higher efficiency and is more applicable to time-varying mobile communication, because no resource-consuming CSI feedback is needed in UL CoMP as illustrated in **Figure 2-9** and **Figure 2-10**. For simplicity, the case of a single UE in a cell is considered (u = 1) in this thesis, which can be easily extended to the case of multiple UEs. In this case, the received signals at the kth BS, the received signal from the entire cooperative set, and the received signal after decoder $\mathbf{U}^H$ are given respectively by (2.1), (2.2), and (2.3), but with $\mathbf{V}_l = \mathbf{V}_l^1$ and $\mathbf{s}_l = \mathbf{s}_l^1$. For all cases, we focus on the scenario that all UEs have equal number of transmit layers, i.e., $d_k = d$, and a linear MMSE receiver is adopted for $\mathbf{F}$ in (2.4). Perfect channel estimation, perfect power control, and negligible timing advanced are assumed as well.

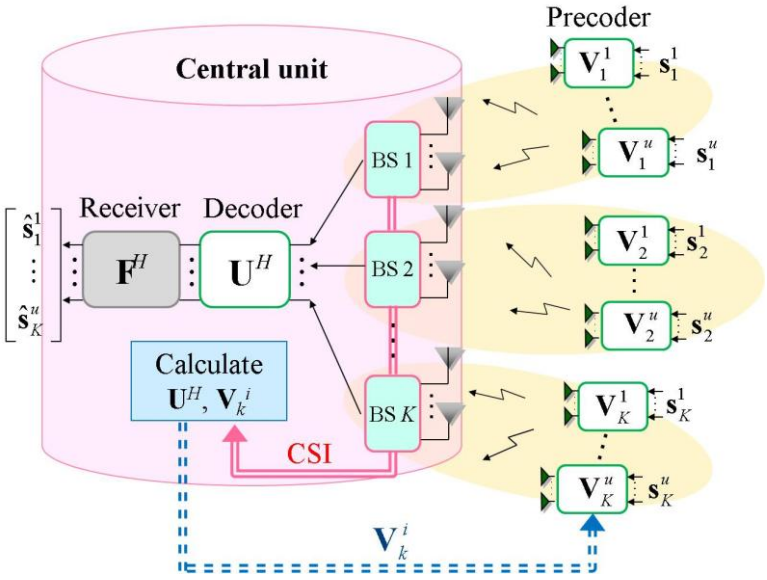

Figure 2-9: Illustration of UL CoMP closed loop communication system

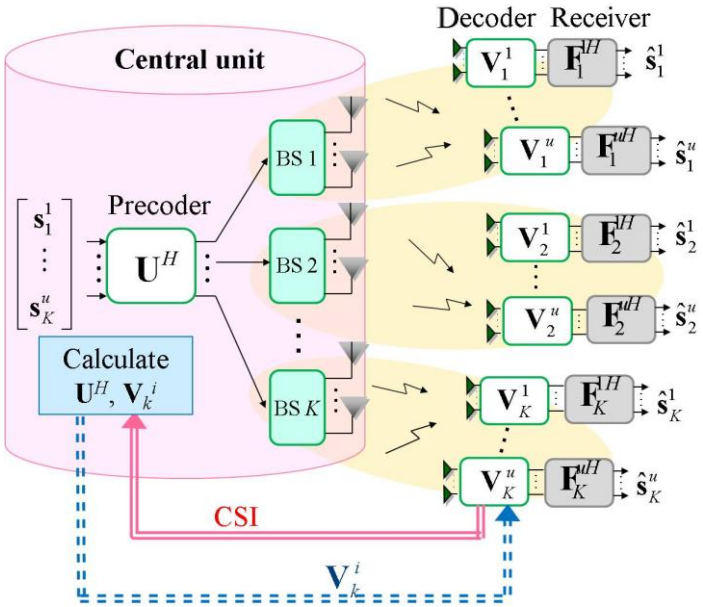

Figure 2-10: Illustration of DL CoMP closed loop communication system

Sum-rate performance is a major performance index in CoMP systems, and it highly depends on the system model considered. In our work, the proposed transceiver schemes are equipped with a linear MMSE receiver; hence the associated achievable sum-rate is calculated according to [11]. When particular precoders and joint decoder are adopted, the maximum achievable sum-rate is calculated according to the equivalent channel matrix in (2.3). That is, in this case, the optimal receiver $\mathbf{F}$ is adopted. The achievable sum-rate employing particular precoders and decoder is depicted as follow:

$$R_{\text{optimal}} = \mathrm{E}_H\left\{\log_2\left(\det\left(\mathbf{I}_{d_T} + R_{\tilde{n}\tilde{n}}^{-1}\tilde{\mathbf{H}}\tilde{\mathbf{H}}^H\right)\right)\right\} \quad (\text{bps/Hz}), \tag{2.6}$$

where $R_{\tilde{n}\tilde{n}} = \mathrm{E}\left\{\tilde{\mathbf{n}}\tilde{\mathbf{n}}^H\right\}$ stands for the correlation matrix of the effective noise $\tilde{\mathbf{n}}$. On the other hand, in our case equipped with linear MMSE receiver (i.e., $\mathbf{F}_{\text{MMSE}}^H = \tilde{\mathbf{H}}^H\left(\tilde{\mathbf{H}}\tilde{\mathbf{H}}^H + R_{\tilde{n}\tilde{n}}\right)^{-1}$), the achievable sum-rate according to (2.4) is given by [11]:

$$R_{\text{MMSE}} = \sum_{a=1}^{K}\sum_{b=1}^{d} \mathrm{E}_H\left\{\log_2\left(1+\tilde{\gamma}_a^b\right)\right\} = \sum_{i=1}^{d_T} \mathrm{E}_H\left\{\log_2\left(1+\gamma_i\right)\right\} \quad (\text{bps/Hz}), \tag{2.7}$$

$$\gamma_i = \frac{1}{\left[\left(\mathbf{I}_{d_T} + \tilde{\mathbf{H}}^H R_{\tilde{n}\tilde{n}}^{-1}\tilde{\mathbf{H}}\right)^{-1}\right]_{i,i}} - 1, \tag{2.8}$$

where we assume each receiver output is decoded independently, and $\tilde{\gamma}_a^b$ is the instantaneous SINR corresponding to the *b*th layer of *a*th user at the output of receiver. In (2.7), $\gamma_i = \tilde{\gamma}_a^b, i = (a-1)\cdot d + b$ is the instantaneous SINR of the *i*th output of receiver corresponding to the *i*th element of $\hat{\mathbf{s}}$, and $d_T = d \cdot K$.

2.3 Interference Alignment in *K*-user Interference Channel

Interference alignment (IA) has recently emerged as a generalized multi-user MIMO technique for the X-channel and *K*-user interference channel scenarios [8]-[9]. The basic idea of IA is to align or compress interference into some limited subspace so the interference can be separated from the desired signal with sufficient degrees of freedom (DoF). The DoF can be provided by multiple antennas, frequency, time, or phase, though multiple-antenna is the most commonly adopted one. Both centralized and distributed IA algorithms have been developed [9],[12]. Distributed IA starts with an arbitrary precoder which induced an optimal decoder at receiver side and then this decoder triggers another algorithm to update the precoder at transmitter side. The algorithm goes back and forth between BSs and user equipments (UEs) to attain interference alignment. Thus distributed IA is more suitable for time division duplex systems and the case with constant channels. In centralized IA, the iterative process is performed by the CU as usually available in CoMP. Thus centralized IA is more

practical for mobile cellular communications. The application of IA in cellular systems has been studied in which multiple UEs are communicating with multiple BSs in distributed CoMP [13]. However, the application of IA to centralized CoMP has not been widely studied. Hence in this thesis, we try to incorporate centralized IA in centralized UL CoMP to achieve better performance.

In the *K*-user interference channel model, there are *K* BSs and *K* UEs, each BS serving a single UE, i.e. $u=1$, as depicted in **Figure 2-11**. The transmitted signal $\mathbf{s}_k$ from UE in *k*th cell is intended for *k*th BS. Each BS processes its own received signal as follows:

$$\tilde{\mathbf{y}}_{k,K\text{-user}} = \mathbf{U}_k^H \sum_{l=1}^{K} \mathbf{H}_{k,l}\mathbf{V}_l\mathbf{s}_l + \mathbf{U}_k^H\mathbf{n}_k \,, \tag{2.9}$$

$$\hat{\mathbf{s}}_{k,K\text{-user}} = \mathbf{F}_k^H\mathbf{U}_k^H \sum_{l=1}^{K} \mathbf{H}_{k,l}\mathbf{V}_l\mathbf{s}_l + \mathbf{F}_k^H\mathbf{U}_k^H\mathbf{n}_k \,, \tag{2.10}$$

where $\mathbf{U}_k^H \in \mathbb{C}^{d_k \times M_r}$ and $\mathbf{F}_k^H \in \mathbb{C}^{d_k \times d_k}$ represent the decoder matrix and receiver matrix, respectively; $\mathbf{V}_l = \mathbf{V}_l^1$ and $\mathbf{s}_l = \mathbf{s}_l^1$ are assumed.

For *K*-user interference channel, IA has proved to be a capacity achieving approach which aligns the interference into some limited subspace so there would be some residual DoF for the desired signal as illustrated in **Figure 2-11**. The design criterion of IA is given as follows [9]-[12] (taking *k*th BS for example):

$$\mathbf{U}_k^H\mathbf{H}_{k,l}\mathbf{V}_l = \mathbf{0}, \forall l \neq k \,, \tag{2.11}$$

$$\text{rank}\left(\mathbf{U}_k^H\mathbf{H}_{k,k}\mathbf{V}_k\right) = d_k . \tag{2.12}$$

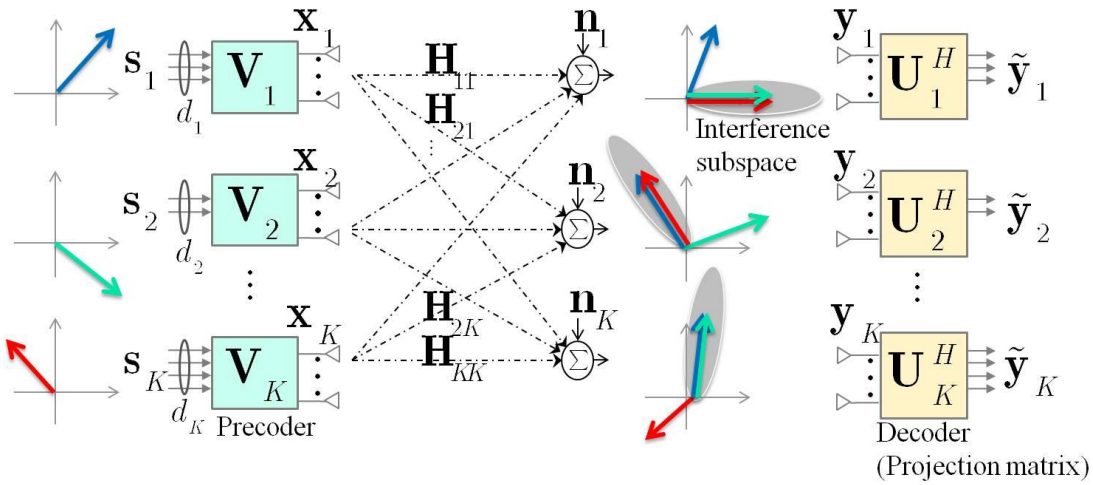

Figure 2-11: Illustration of IA in *K*-user interference channel

Several approaches have been proposed to achieve these criteria, e.g. minimum leakage (Min Leakage-IA), maximum SINR (Max SINR-IA) and maximum sum-rate [14]. Min Leakage-IA and Max SINR-IA are two popular iterative IA algorithms [9], [12] which will be adopted in UL CoMP and their performance will be evaluated in our work. These two iterative IA algorithms have advantage of flexibility and can be implemented with various transceiver setups [9], [12]. The iterative procedure based on UL-DL duality is listed in **Table 2-1**.

Max SINR-IA considers the impact of interference and noise jointly to reach a better compromise at low to moderate SNR by maximizing the SINR of the *i*th layer corresponding to the *k*th user, SINR_k^i ($\forall i \in \{1,2,\cdots,d_k\}$, $\forall k \in \{1,2,\cdots,K\}$). Each column of decoders is calculated by the algorithm:

$$\max_{\mathbf{U}_k^{(i)}} \mathrm{SINR}_k^i = \max_{\mathbf{U}_k^{(i)}} \left(\frac{\mathbf{U}_k^{(i)H} \mathbf{H}_{k,k} \mathbf{V}_k^{(i)} \mathbf{V}_k^{(i)H} \mathbf{H}_{k,k}^H \mathbf{U}_k^{(i)}}{\mathbf{U}_k^{(i)H} \mathbf{B}_k^{(i)} \mathbf{U}_k^{(i)}} \right), \tag{2.13}$$

$$\mathbf{B}_k^{(i)} = \sum_l \sum_d \mathbf{H}_{k,l} \mathbf{V}_l^{(d)} \mathbf{V}_l^{(d)H} \mathbf{H}_{k,l}^H - \mathbf{H}_{k,k} \mathbf{V}_k^{(i)} \mathbf{V}_k^{(i)H} \mathbf{H}_{k,k}^H + N_0 \mathbf{I}. \tag{2.14}$$

The optimal $\mathbf{U}_k^{(i)}$ for (2.13) is given by

$$\mathbf{U}_k^{(i)} = \frac{\left(\mathbf{B}_k^{(i)}\right)^{-1}\mathbf{H}_{k,k}\mathbf{V}_k^{(i)}}{\left\|\left(\mathbf{B}_k^{(i)}\right)^{-1}\mathbf{H}_{k,k}\mathbf{V}_k^{(i)}\right\|}. \tag{2.15}$$

With $\mathbf{U}_k$ obtained from previous step, each column of precoders $\mathbf{V}_k$ is calculated based on virtual DL system model by the algorithm:

$$\max_{\mathbf{v}_k^{(i)}} \overline{\mathrm{SINR}}_k^{\,i} = \max_{\mathbf{v}_k^{(i)}} \left(\frac{\rho_k^2 \mathbf{V}_k^{(i)H}\mathbf{H}_{k,k}^H\mathbf{U}_k^{(i)}\mathbf{U}_k^{(i)H}\mathbf{H}_{k,k}\mathbf{V}_k^{(i)}}{\mathbf{V}_k^{(i)H}\mathbf{A}_k^{(i)}\mathbf{V}_k^{(i)}} \right), \tag{2.16}$$

$$\mathbf{A}_k^{(i)} = \sum_l \sum_d \rho_l^2 \mathbf{H}_{l,k}^H \mathbf{U}_l^{(d)}\mathbf{U}_l^{(d)H}\mathbf{H}_{l,k} - \rho_k^2 \mathbf{H}_{k,k}^H \mathbf{U}_k^{(i)}\mathbf{U}_k^{(i)H}\mathbf{H}_{k,k} + N_0\mathbf{I}, \tag{2.17}$$

where ρ_l is chosen to satisfy $\mathrm{tr}(\rho_l^2 \mathbf{U}_l\mathbf{U}_l^H) = P$. The optimal $\mathbf{V}_k^{(i)}$ for (2.16) is given by

Table 2-1: Iterative procedure of Max SINR-IA and Min Leakage-IA

Step 1.	Start with arbitrary precoders $\mathbf{V}_k$, $\forall k \in \{1, 2, \ldots, K\}$
Step 2.	Compute decoders $\mathbf{U}_k$ using Max SINR-IA or Min Leakage-IA with $\mathbf{V}_k$ obtained from previous step, $\forall k \in \{1, 2, \ldots, K\}$.
Step 3.	Based on virtual DL system model, compute precoder $\mathbf{V}_k$ using Max SINR-IA or Min Leakage-IA with $\mathbf{U}_k$ obtained from previous step, $\forall k \in \{1, 2, \ldots, \mathrm{K}\}$.
Step 4.	Go back to **Step 2** unless the number of iterations reaches a predefined limit.

$$\mathbf{V}_k^{(i)} = \mu_k \frac{\left(\mathbf{A}_k^{(i)}\right)^{-1}\mathbf{H}_{k,k}^H\mathbf{U}_k^{(i)}}{\left\|\left(\mathbf{A}_k^{(i)}\right)^{-1}\mathbf{H}_{k,k}^H\mathbf{U}_k^{(i)}\right\|}, \tag{2.18}$$

where μ_k is chosen to satisfy $\mathrm{tr}(\mathbf{V}_k\mathbf{V}_k^H) = P$. The iterative procedure of Max SINR-IA is listed in **Table 2-1**.

On the other hand, Min Leakage-IA focuses on (2.11) by minimizing the total interference leakage corresponding to the *k*th user while assuming (2.12) is automatically satisfied. Each decoder is calculated by the algorithm:

$$\min_{\mathbf{U}_k} \operatorname{tr}\left(\mathbf{U}_k^H \mathbf{Q}_k \mathbf{U}_k\right), \tag{2.19}$$

$$\mathbf{Q}_k = \sum_{l \neq k} \mathbf{H}_{k,l} \mathbf{V}_l \mathbf{V}_l^H \mathbf{H}_{k,l}^H, \tag{2.20}$$

which yields

$$\mathbf{U}_k^{(d)} = \operatorname{eig}_d[\mathbf{Q}_k], \tag{2.21}$$

where $\operatorname{eig}_d[\mathbf{A}]$ represents the eigenvector corresponding to the dth smallest eigenvalue of $\mathbf{A}$. With $\mathbf{U}_k$ obtained from previous step, each precoders $\mathbf{V}_k$ is calculated based on virtual DL system model by the algorithm:

$$\min_{\mathbf{V}_k} \operatorname{tr}\left(\mathbf{V}_k^H \tilde{\mathbf{Q}}_k \mathbf{V}_k\right), \tag{2.22}$$

$$\tilde{\mathbf{Q}}_k = \sum_{l \neq k} \rho_l^2 \mathbf{H}_{l,k}^H \mathbf{U}_l \mathbf{U}_l^H \mathbf{H}_{l,k}, \tag{2.23}$$

where ρ_l is chosen to satisfy $\operatorname{tr}(\rho_l^2 \mathbf{U}_l \mathbf{U}_l^H) = P$. (2.22) and (2.23) yield

$$\mathbf{V}_k^{(d)} = \mu_k \cdot \operatorname{eig}_d[\tilde{\mathbf{Q}}_k]. \tag{2.24}$$

where μ_k is chosen to satisfy $\operatorname{tr}(\mathbf{V}_k \mathbf{V}_k^H) = P$. The iterative procedure of Min Leakage-IA is listed in **Table 2-1**.

2.4 Summary

To cope with the interference issues in modern mobile communication systems and to further enhance the system performance, CoMP has been proposed as a key

technique. In this chapter, the infrastructure and classification of CoMP are firstly provided, and then the closed loop centralized UL CoMP system adopted in this thesis and its associated mathematical system model are introduced. Moreover, the sum-rate as the performance index is described as well. Finally, a promising technique, interference alignment, aiming at interference mitigation in *K*-user interference channel is illustrated. The basic idea of IA will be incorporated into one of our proposed transceiver designs.

Chapter 3

Interference Alignment (IA) Aided Transceiver Design

The interference from other cells which severely degrade the system performance is a crucial factor in modern wireless cellular communication systems and should be carefully managed. To cope with the issues caused by interference such as inconsistent service quality at cell-edge, poor cell coverage, and inferior throughput and to further improve the system efficiency, a promising technique, coordinated multipoint (CoMP) transmission and reception, is developed. In such scenario, the transceiver design based on the full BS cooperation is a critical issue.

In this thesis, two centralized UL CoMP transceiver schemes with multiple transmit antennas, receive antennas, and transmit layers are proposed; the one which incorporates the idea of interference management is provided in this chapter. Interference alignment is a new emerging interference management technique which is developed based on *K*-user interference channel structure, and its superior advantage for interference mitigation has been widely evaluated and discussed in *K*-user interference channel.

The organization of this chapter is shown below. The motivation of the proposed IA aided UL CoMP transceiver scheme is given in section 3.1. In section 3.2, we introduce the incorporation of IA in UL CoMP based on two popular iterative IA

algorithms, Min Leakage-IA and Max SINR-IA provided in [9], [12], and their performances will be evaluated. After the investigation in section 3.2, we propose an IA aided UL CoMP transceiver scheme based on the full cooperation at BSs in section 3.3. Then the numerical evaluation and discussion are provided in section 3.4. Finally, we summarize this chapter in section 3.5

3.1 Motivation

In an interference limited communication environment, there are two typical interference management methods: 1) to decode the desired signal and interference simultaneously and 2) to separate the desired signal from interference by allocating orthogonal/independent physical resource (time, frequency, space, etc.). It is reasonable to infer that incorporating the concept of second approach into the first one can have great potential for dealing with the interference issues.

The inter cell interference which is often treated as noise in the case without BS cooperation is now decodable along with the desired signal at CU owing to the full BS cooperation provided by centralized UL CoMP as illustrated in (2.3). That is the first interference management method mentioned above is provided by centralized UL CoMP. On the other hand, interference alignment is belonging to the second interference management method, and it tries to align the interference into some limited subspace that is independent to the desired signal.

Considering the capability for interference mitigation provided by the two typical interference management methods, we combine the two methods in our first transceiver design which leads to equivalent channel matrix (2.5) reformulation in our work. Hence we aim to capture the basic idea of IA in our precoder and decoder design so that a well-behaved equivalent channel matrix can be obtained.

3.2 Incorporation of IA in UL CoMP

In *K*-user interference channel, IA intends to align interference at each terminal that inter-user/inter-cell interference can be separated from desired signal and then be alleviated successfully. In this work, we attempt to incorporate IA in our UL CoMP transceiver design (precoder and decoder design as illustrated in section 2.2) where the interference is aligned and then suppressed at the output of joint decoder $\mathbf{U}^H$ based on two popular iterative IA algorithms, Min Leakage-IA and Max SINR-IA provided in [9], [12]. Owing to the intention of interference alignment and mitigation, the residual interference for each layer/user at the output of decoder will be minimized, and a near diagonal /block diagonal effective channel matrix in (2.3) and (2.4) is formed.

According to the system model of centralized UL CoMP depicted in (2.3) and the design principle of IA in *K*-user interference channel demonstrated in (2.11) and (2.12), the UL CoMP transceiver design which incorporates IA is based on the criteria shown below (taking *k*th BS for example, $\forall k \in \{1,2,\ldots,K\}$):

$$\left(\mathbf{U}_{(k-1)d+1}^{k\times d} \right)^H \mathbf{H}_l \mathbf{V}_l = 0, \forall l \neq k\,, \tag{3.1}$$

$$\operatorname{rank}\left(\left(\mathbf{U}_{(k-1)d+1}^{k\times d} \right)^H \mathbf{H}_k \mathbf{V}_k \right) = d\,, \tag{3.2}$$

where $\mathbf{H}_l = [\mathbf{H}_{1,l}^T, \mathbf{H}_{2,l}^T, \ldots, \mathbf{H}_{K,l}^T]^T \in \mathbb{C}^{KM_r \times M_t}$. The main difference between IA in *K*-user interference channel and IA in centralized CoMP is that the latter incorporates full cooperation between BSs for computing the decoders at the BSs. In order to achieve these criteria, we embrace the basic idea of the following two iterative IA approaches developed in *K*-user interference channel: Min Leakage-IA and Max

SINR-IA [9], [12]. In the rest of this thesis, the UL CoMP transceiver schemes assisted with Min Leakage-IA and Max SINR-IA are called Min Leakage-UL CoMP and Max SINR-UL CoMP, respectively. The two UL CoMP transceiver schemes both involve an iterative procedure based on UL-DL duality, and each iteration consists of two stages: 1) to calculate the joint decoder and 2) to compute the precoders according to the corresponding virtual DL CoMP system.

In regard to Min Leakage-IA aided Uplink CoMP (Min Leakage-UL CoMP) we obtain the modified optimization problem for joint decoder $\mathbf{U}$ from Min Leakage-IA depicted in (2.19) (taking *k*th BS for example, $\forall k \in \{1,2,\ldots,K\}$):

$$\min_{\{\mathbf{U}\}_{(k-1)d+1}^{k\cdot d}} \operatorname{tr}\left(\{\mathbf{U}\}_{(k-1)d+1}^{k\cdot d}{}^{H} \mathbf{Q}_k \{\mathbf{U}\}_{(k-1)d+1}^{k\cdot d}\right), \tag{3.3}$$

where $\mathbf{Q}_k = \sum_{l\neq k} \mathbf{H}_l \mathbf{V}_l \mathbf{V}_l^H \mathbf{H}_l^H$, which yields

$$\mathbf{U}^{((k-1)d+l)} = \operatorname{eig}_l[\mathbf{Q}_k], \forall l \in \{1,2,\ldots,d\}. \tag{3.4}$$

We can obtain precoders by the virtual DL CoMP system. Minimizing the total interference leakage at the UE in *k*th cell gives

$$\min_{\mathbf{V}_k} \operatorname{tr}\left(\mathbf{V}_k^H \tilde{\mathbf{Q}}_k \mathbf{V}_k\right), \tag{3.5}$$

where $\tilde{\mathbf{Q}}_k = \sum_{l\neq k} \rho^2 \mathbf{H}_k^H \{\mathbf{U}\}_{(l-1)d+1}^{l\cdot d} \{\mathbf{U}\}_{(l-1)d+1}^{l\cdot d}{}^{H} \mathbf{H}_k$, and ρ is chosen to satisfy $\operatorname{tr}(\rho^2 \mathbf{U}\mathbf{U}^H) = K \cdot P$. This yields

$$\mathbf{V}_k^{(d)} = \mu_k \cdot \operatorname{eig}_d[\tilde{\mathbf{Q}}_k], \forall l \in \{1,2,\ldots,d\}, \tag{3.6}$$

where μ_k is chosen to satisfy $\operatorname{tr}(\mathbf{V}_k \mathbf{V}_k^H) = P$. In this UL CoMP scheme, the Min Leakage mechanism tries to build a block diagonal effective channel matrix, $\tilde{\mathbf{H}} = \mathbf{U}^H \mathbf{H} \mathbf{V}$. The iterative procedure of Min Leakage-UL CoMP is listed in **Table 3-1**.

On the other hand, Max SINR-IA aided Uplink CoMP (Max SINR-UL CoMP) try

to maximize the SINR corresponding to different layers (data streams) at the output of decoder. Taking into account system model provided by (2.3) and the basic idea of Max SINR-IA, we reformulate (2.13) into the following objective function which aims at maximizing the SINR of the *i*th layer corresponding to the *k*th user, SINR_k^i ($\forall i \in \{1,2,\cdots,d\}$, $\forall k \in \{1,2,\cdots,K\}$); each column of decoders is calculated by the algorithm:

$$\max_{\mathbf{U}^{((k-1)d+i)}} \mathrm{SINR}_k^i = \max_{\mathbf{U}^{((k-1)d+i)}} \left(\frac{\mathbf{U}^{((k-1)d+i)H} \mathbf{H}_k \mathbf{V}_k^{(i)} \mathbf{V}_k^{(i)H} \mathbf{H}_k^H \mathbf{U}^{((k-1)d+i)}}{\mathbf{U}^{((k-1)d+i)H} \mathbf{B}_k^{(i)} \mathbf{U}^{((k-1)d+i)}} \right), \tag{3.7}$$

$$\mathbf{B}_k^{(i)} = \sum_l \sum_t \mathbf{H}_l \mathbf{V}_l^{(t)} \mathbf{V}_l^{(t)H} \mathbf{H}_l^H - \mathbf{H}_k \mathbf{V}_k^{(i)} \mathbf{V}_k^{(i)H} \mathbf{H}_k^H + N_0 \mathbf{I}, \tag{3.8}$$

which yields:

$$\mathbf{U}^{((k-1)d+i)} = \frac{\left(\mathbf{B}_k^{(i)}\right)^{-1} \mathbf{H}_k \mathbf{V}_k^{(i)}}{\left\| \left(\mathbf{B}_k^{(i)}\right)^{-1} \mathbf{H}_k \mathbf{V}_k^{(i)} \right\|}, \tag{3.9}$$

$\forall i \in \{1,2,\cdots,d\}, \forall k \in \{1,2,\cdots,K\}$, where $\mathbf{U}$ is the joint decoder matrix as described in (2.3). For the precoder design, we consider the corresponding virtual DL system model with which SINR_k^i is maximized: $\forall i \in \{1,2,\ldots,d\}$, $\forall k \in \{1,2,\ldots,K\}$

$$\max_{\mathbf{v}_k^{(i)}} \overline{\mathrm{SINR}}_k^i = \max_{\mathbf{v}_k^{(i)}} \left(\frac{\rho^2 \mathbf{V}_k^{(i)H} \mathbf{H}_k^H \mathbf{U}^{((k-1)d+i)} \mathbf{U}^{((k-1)d+i)H} \mathbf{H}_k \mathbf{V}_k^{(i)}}{\mathbf{V}_k^{(i)H} \tilde{\mathbf{B}}_k^{(i)} \mathbf{V}_k^{(i)}} \right), \tag{3.10}$$

$$\begin{aligned} \tilde{\mathbf{B}}_k^{(i)} = & \sum_l \sum_t \rho^2 \mathbf{H}_k^H \mathbf{U}^{((l-1)d+t)} \mathbf{U}^{((l-1)d+t)H} \mathbf{H}_k \\ & - \rho^2 \mathbf{H}_k^H \mathbf{U}^{((k-1)d+i)} \mathbf{U}^{((k-1)d+i)H} \mathbf{H}_k + N_0 \mathbf{I} \end{aligned}, \tag{3.11}$$

where ρ is chosen to satisfy $\mathrm{tr}(\rho^2 \mathbf{U}\mathbf{U}^H) = K \cdot P$. Hence (3.10) yields

$$\mathbf{V}_k^{(i)} = \mu_k \frac{\left(\tilde{\mathbf{B}}_k^{(i)}\right)^{-1} \mathbf{H}_k^H \mathbf{U}^{((k-1)d+i)}}{\left\| \left(\tilde{\mathbf{B}}_k^{(i)}\right)^{-1} \mathbf{H}_k^H \mathbf{U}^{((k-1)d+i)} \right\|}, \tag{3.12}$$

where μ_k is chosen to satisfy $\mathrm{tr}(\mathbf{V}_k \mathbf{V}_k^H) = P$. In this UL CoMP scheme, the Max SINR-IA algorithm plays an importance role to convert the original channel into a more tractable effective channel, $\tilde{\mathbf{H}} = \mathbf{U}^H \mathbf{H} \mathbf{V}$, which is nearly diagonal. The detail of this iterative algorithm is summarized in **Table 3-1**.

Table 3-1: Iterative procedure of Min Leakage-UL CoMP and Max SINR-UL CoMP

Step 1.	Start with arbitrary precoders $\mathbf{V}_k$, $\forall k \in \{1, 2, \ldots, K\}$
Step 2.	Compute the joint decoder **U** using Min Leakage-UL CoMP (3.4) or Max SINR-UL CoMP (3.9) with $\mathbf{V}_k$ obtained from previous step, $\forall k \in \{1, 2, \ldots, K\}$.
Step 3.	Based on virtual DL system model, compute precoder $\mathbf{V}_k$ using Min Leakage-UL CoMP (3.6) or Max SINR-UL CoMP (3.12) with **U** obtained from previous step, $\forall k \in \{1, 2, \ldots, \mathrm{K}\}$.
Step 4.	Go back to **Step 2** unless the number of iterations reaches a predefined limit.

After the derivation of the two IA aided Uplink CoMP schemes, the achievable sum-rate performance comparison is provided by numerical simulation as shown in **Figure 3-1**. In our simulation, linear MMSE receiver is adopted, and sum-rate performance is calculated according to (2.7) as mentioned in section 2.2. The simulation results in this section are obtained by averaging over 100 independent channel realizations, and 20 iterations were performed for each iterative algorithm. The entries of the associated channel matrix are assumed i.i.d. complex Gaussian with unit

variance. Three BSs in one cooperative group and one UE in the coverage of each BS (K = 3, u = 1) are considered. All BSs are equipped with M_r = 4 antennas, and all UEs are equipped with M_t = 4 antennas. All UEs have equal number of transmit signals, i.e., d = 2.

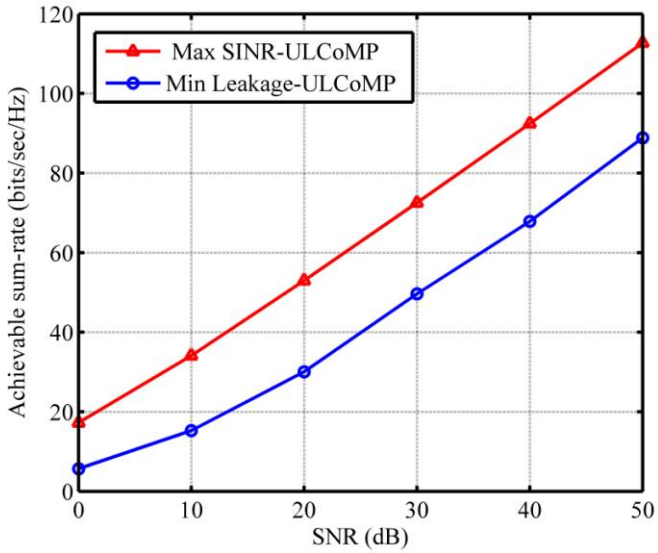

Figure 3-1: Sum-rate performance of Min Leakage-UL CoMP and Max SINR-UL CoMP with K=3, M_t=4, M_r=4, d=2, and no. of iterations=20

The simulation result shows that Max SINR-UL CoMP significantly outperforms Min Leakage-UL CoMP. The major reason is that Min Leakage-UL CoMP mechanism tries to minimize the interference leakage but assumes (3.2) is automatically satisfied. That is only the interference effect is considered, and there is no guarantee for the detection quality of the desired signal. On the other hand, the Max SINR-UL CoMP algorithm preserves a good compromise between interference and received power of desired signal because it takes both into account. As a potential solution to manage the interference issue and to further improve the system performance, the basic idea of Max SINR-ULCoMP is embraced in our proposed IA aided UL CoMP transceiver

scheme in section 3.3.

3.3 Proposed IA Aided Transceiver in UL CoMP

According to the discussion and simulation result in section 3.2, it is found that Max SINR-UL CoMP achieves better sum-rate performance compared to Min Leakage-UL CoMP, because the first one aided by Max SINR-IA preserves a good compromise between interference and received power of desired signal. In terms of effective channel matrix $\tilde{\mathbf{H}}$, a near diagonal effective channel matrix is accomplished by Max SINR-ULCoMP, since the SINR maximization will somehow suppress the off-diagonal terms of the effective channel matrix. However, since the SINR maximization is executed layer by layer, the SINR performance achieved by each layer might be highly diverse leading to a poor-conditioned effective channel matrix. To improve the condition of the effective channel matrix, it is desired to further balance the layer SINR at the decoder output. Therefore we attempt to propose an IA aided UL CoMP transceiver that can achieve good trade-off between interference issue and received power of desired signal by SINR maximization, and can balance the SINR of each layer at the output of decoder.

The proposed IA aided UL CoMP transceiver is achieved by maximizing the product of instantaneous SINRs for each layer (per-layer SINR), which in turn attempts to increase each per-layer SINR and to reduce the difference between the per-layer SINRs at the output of decoder. Namely, the proposed IA aided UL CoMP scheme aims at maximizing the function shown below:

$$\prod_{k',i'} \mathrm{SINR}_{k'}^{i'} = \prod_{k',i'} \frac{\mathbf{U}^{((k'-1)d+i')H}\mathbf{H}_{k'}\mathbf{V}_{k'}^{(i')}\mathbf{V}_{k'}^{(i')H}\mathbf{H}_{k'}^{H}\mathbf{U}^{((k'-1)d+i')}}{\mathbf{U}^{((k'-1)d+i')H}\mathbf{B}_{k'}^{(i')}\mathbf{U}^{((k'-1)d+i')}}, \tag{3.13}$$

$$\mathbf{B}_{k'}^{(i')} = \sum_{l}\sum_{t}\mathbf{H}_{l}\mathbf{V}_{l}^{(t)}\mathbf{V}_{l}^{(t)H}\mathbf{H}_{l}^{H} - \mathbf{H}_{k'}\mathbf{V}_{k'}^{(i')}\mathbf{V}_{k'}^{(i')H}\mathbf{H}_{k'}^{H} + N_0\mathbf{I}, \tag{3.14}$$

where SINR_k^i is the SINR corresponding to the *i*th layer of the *k*th user at the output of decoder as illustrated in **Figure 3-2** ($\forall i \in \{1,2,\cdots,d\}$, $\forall k \in \{1,2,\cdots,K\}$). The proposed IA aided UL CoMP transceiver scheme involves an iterative procedure as shown in **Figure 3-3**, and each iteration consists of two stages: 1) to calculate the joint decoder and 2) to compute the precoders.

In the first stage, each column of the joint decoder is computed successively by the algorithm shown below:

$$\max_{\mathbf{U}^{((k-1)d+i)}} \prod_{k',i'} \mathrm{SINR}_{k'}^{i'} = \max_{\mathbf{U}^{((k-1)d+i)}} \prod_{k',i'} \frac{\mathbf{U}^{((k'-1)d+i')H}\mathbf{H}_{k'}\mathbf{V}_{k'}^{(i')}\mathbf{V}_{k'}^{(i')H}\mathbf{H}_{k'}^{H}\mathbf{U}^{((k'-1)d+i')}}{\mathbf{U}^{((k'-1)d+i')H}\mathbf{B}_{k'}^{(i')}\mathbf{U}^{((k'-1)d+i')}}, \quad (3.15)$$

$$\mathbf{B}_{k'}^{(i')} = \sum_{l}\sum_{t}\mathbf{H}_l\mathbf{V}_l^{(t)}\mathbf{V}_l^{(t)H}\mathbf{H}_l^{H} - \mathbf{H}_{k'}\mathbf{V}_{k'}^{(i')}\mathbf{V}_{k'}^{(i')H}\mathbf{H}_{k'}^{H} + N_0\mathbf{I}, \quad (3.16)$$

where $\forall i \in \{1,2,\cdots,d\}$ and $\forall k \in \{1,2,\cdots,K\}$. The objective function mentioned above is equal to the criterion,

$$\max_{\mathbf{U}^{((k-1)d+i)}} \frac{\mathbf{U}^{((k-1)d+i)H}\mathbf{H}_k\mathbf{V}_k^{(i)}\mathbf{V}_k^{(i)H}\mathbf{H}_k^{H}\mathbf{U}^{((k-1)d+i)}}{\mathbf{U}^{((k-1)d+i)H}\mathbf{B}_k^{(i)}\mathbf{U}^{((k-1)d+i)}}, \quad (3.17)$$

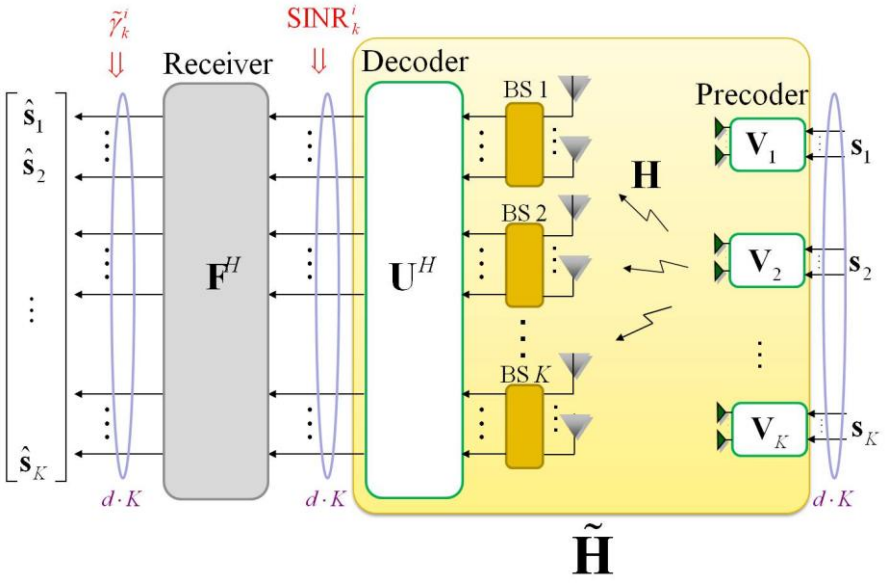

Figure 3-2: Illustration of centralized UL CoMP transceiver scheme, SINR_k^i, and $\tilde{\gamma}_k^i$

which yields the same results as obtained in Max SINR-UL CoMP:

$$\mathbf{U}^{((k-1)d+i)} = \frac{\left(\mathbf{B}_k^{(i)}\right)^{-1}\mathbf{H}_k\mathbf{V}_k^{(i)}}{\left\|\left(\mathbf{B}_k^{(i)}\right)^{-1}\mathbf{H}_k\mathbf{V}_k^{(i)}\right\|}, \tag{3.18}$$

$\forall i \in \{1,2,\cdots,d\}, \forall k \in \{1,2,\cdots,K\}$.

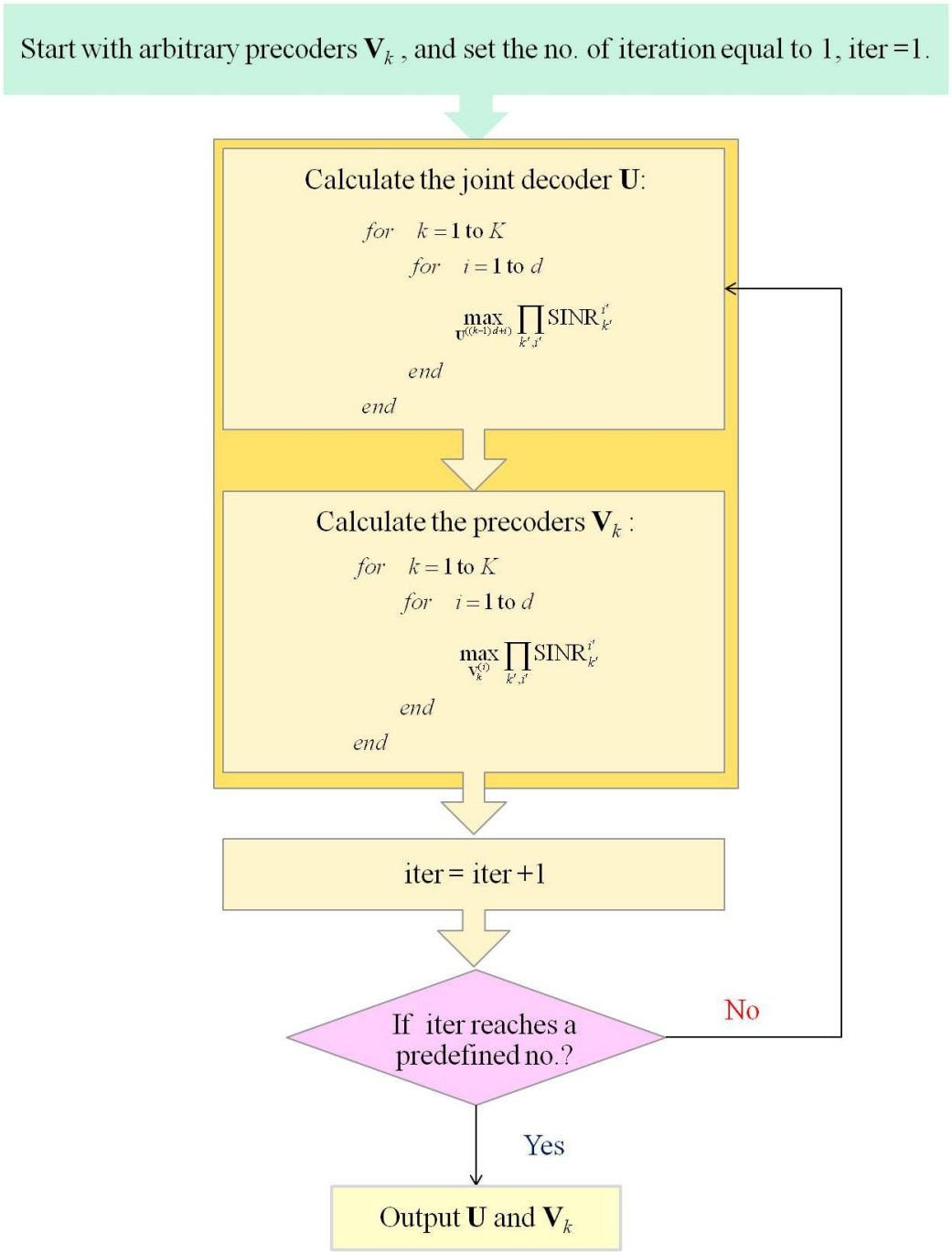

Figure 3-3: Flow chart of the proposed IA aided UL CoMP scheme

In the second stage, each column of the precoders is computed successively by the algorithm shown below:

$$\max_{\mathbf{v}_k^{(i)}} \prod_{k',i'} \mathrm{SINR}_{k'}^{i'} = \max_{\mathbf{v}_k^{(i)}} \prod_{k',i'} \frac{\mathbf{U}^{((k'-1)d+i')H}\mathbf{H}_{k'}\mathbf{V}_{k'}^{(i')}\mathbf{V}_{k'}^{(i')H}\mathbf{H}_{k'}^{H}\mathbf{U}^{((k'-1)d+i')}}{\mathbf{U}^{((k'-1)d+i')H}\mathbf{B}_{k'}^{(i')}\mathbf{U}^{((k'-1)d+i')}}, \quad (3.19)$$

$$\mathbf{B}_{k'}^{(i')} = \sum_{l}\sum_{t}\mathbf{H}_l\mathbf{V}_l^{(t)}\mathbf{V}_l^{(t)H}\mathbf{H}_l^{H} - \mathbf{H}_{k'}\mathbf{V}_{k'}^{(i')}\mathbf{V}_{k'}^{(i')H}\mathbf{H}_{k'}^{H} + N_0\mathbf{I}, \quad (3.20)$$

where $\forall i \in \{1,2,\cdots,d\}$ and $\forall k \in \{1,2,\cdots,K\}$. The objective function mentioned above is equal to the one shown below:

$$\begin{aligned}
&\max_{\mathbf{v}_k^{(i)}} \frac{\mathbf{U}^{((k-1)d+i)H}\mathbf{H}_k\mathbf{V}_k^{(i)}\mathbf{V}_k^{(i)H}\mathbf{H}_k^{H}\mathbf{U}^{((k-1)d+i)}}{\prod_{\substack{k',i'\\(k',i')\neq(k,i)}} \mathbf{U}^{((k'-1)d+i')H}\mathbf{B}_{k'}^{(i')}\mathbf{U}^{((k'-1)d+i')}} \\
\Leftrightarrow &\max_{\mathbf{v}_k^{(i)}} \frac{\mathbf{V}_k^{(i)H}\mathbf{H}_k^{H}\mathbf{U}^{((k-1)d+i)}\mathbf{U}^{((k-1)d+i)H}\mathbf{H}_k\mathbf{V}_k^{(i)}}{\prod_{\substack{k',i'\\(k',i')\neq(k,i)}} \mathbf{U}^{((k'-1)d+i')H}\left(\sum_{\substack{l\in1,\cdots K,t\in1,\cdots d\\(l,t)\neq(k',i')\\(l,t)\neq(k,i)}}\mathbf{H}_l\mathbf{V}_l^{(t)}\mathbf{V}_l^{(t)H}\mathbf{H}_l^{H} + \mathbf{H}_k\mathbf{V}_k^{(i)}\mathbf{V}_k^{(i)H}\mathbf{H}_k^{H} + N_0\mathbf{I}\right)\mathbf{U}^{((k'-1)d+i')}} \\
\Leftrightarrow &\max_{\mathbf{v}_k^{(i)}} \frac{\mathbf{V}_k^{(i)H}\mathbf{H}_k^{H}\mathbf{U}^{((k-1)d+i)}\mathbf{U}^{((k-1)d+i)H}\mathbf{H}_k\mathbf{V}_k^{(i)}}{\prod_{\substack{k',i'\\(k',i')\neq(k,i)}} \left(\begin{array}{l}\sum_{\substack{l\in1,\cdots K,t\in1,\cdots d\\(l,t)\neq(k',i')\\(l,t)\neq(k,i)}}\mathbf{U}^{((k'-1)d+i')H}\mathbf{H}_l\mathbf{V}_l^{(t)}\mathbf{V}_l^{(t)H}\mathbf{H}_l^{H}\mathbf{U}^{((k'-1)d+i')} \\ +\mathbf{U}^{((k'-1)d+i')H}\mathbf{H}_k\mathbf{V}_k^{(i)}\mathbf{V}_k^{(i)H}\mathbf{H}_k^{H}\mathbf{U}^{((k'-1)d+i')} \\ +N_0\mathbf{U}^{((k'-1)d+i')H}\mathbf{U}^{((k'-1)d+i')}\end{array}\right)} \\
\Leftrightarrow &\max_{\mathbf{v}_k^{(i)}} \frac{\mathbf{V}_k^{(i)H}\mathbf{H}_k^{H}\mathbf{U}^{((k-1)d+i)}\mathbf{U}^{((k-1)d+i)H}\mathbf{H}_k\mathbf{V}_k^{(i)}}{\prod_{\substack{k',i'\\(k',i')\neq(k,i)}} \left(\mathbf{V}_k^{(i)H}\mathbf{H}_k^{H}\mathbf{U}^{((k'-1)d+i')}\mathbf{U}^{((k'-1)d+i')H}\mathbf{H}_k\mathbf{V}_k^{(i)} + \Psi_{k',i'}\right)}
\end{aligned}, \quad (3.21)$$

$$\Psi_{k',i'} = \sum_{\substack{l\in1,\cdots K,t\in1,\cdots d\\(l,t)\neq(k',i')\\(l,t)\neq(k,i)}} \mathbf{U}^{((k'-1)d+i')H}\mathbf{H}_l\mathbf{V}_l^{(t)}\mathbf{V}_l^{(t)H}\mathbf{H}_l^{H}\mathbf{U}^{((k'-1)d+i')} + N_0\mathbf{U}^{((k'-1)d+i')H}\mathbf{U}^{((k'-1)d+i')}. \quad (3.22)$$

We assume $\mathbf{V}_k^{(i)H}\mathbf{V}_k^{(i)} = P/d$, so (3.21) turns to

$$\max_{\mathbf{V}_k^{(i)H}} \frac{\mathbf{V}_k^{(i)H}\mathbf{H}_k^H\mathbf{U}^{((k-1)d+i)}\mathbf{U}^{((k-1)d+i)H}\mathbf{H}_k\mathbf{V}_k^{(i)}}{\prod_{\substack{k',i' \\ (k',i')\neq(k,i)}} \left(\mathbf{V}_k^{(i)H}\mathbf{E}_{k',i'}\mathbf{\Lambda}_{k',i'}\mathbf{E}_{k',i'}^H\mathbf{V}_k^{(i)} + \Psi_{k',i'}\mathbf{V}_k^{(i)H}\mathbf{V}_k^{(i)}\cdot d/P\right)}, \tag{3.23}$$

where $\mathbf{E}_{k',i'}\mathbf{\Lambda}_{k',i'}\mathbf{E}_{k',i'}^H$ is the eigenvalue decomposition of $\mathbf{H}_k^H\mathbf{U}^{((k'-1)d+i')}\mathbf{U}^{((k'-1)d+i')H}\mathbf{H}_k$, $\mathbf{E}_{k',i'}\mathbf{E}_{k',i'}^H = \mathbf{I}$, and $\mathbf{\Lambda}_{k',i'} = diag\begin{bmatrix}\alpha_{k',i'} & 0 & \cdots & 0\end{bmatrix}$. Therefore (3.23) equals:

$$\begin{aligned}
&\max_{\mathbf{V}_k^{(i)}} \frac{\mathbf{V}_k^{(i)H}\mathbf{H}_k^H\mathbf{U}^{((k-1)d+i)}\mathbf{U}^{((k-1)d+i)H}\mathbf{H}_k\mathbf{V}_k^{(i)}}{\prod_{\substack{k',i' \\ (k',i')\neq(k,i)}} \left(\mathbf{V}_k^{(i)H}\mathbf{E}_{k',i'}\mathbf{\Lambda}_{k',i'}\mathbf{E}_{k',i'}^H\mathbf{V}_k^{(i)} + \Psi_{k',i'}\mathbf{V}_k^{(i)H}\mathbf{E}_{k',i'}\mathbf{I}\mathbf{E}_{k',i'}^H\mathbf{V}_k^{(i)}\cdot d/P\right)} \\
\Leftrightarrow &\max_{\mathbf{V}_k^{(i)}} \frac{\mathbf{V}_k^{(i)H}\mathbf{H}_k^H\mathbf{U}^{((k-1)d+i)}\mathbf{U}^{((k-1)d+i)H}\mathbf{H}_k\mathbf{V}_k^{(i)}}{\prod_{\substack{k',i' \\ (k',i')\neq(k,i)}} \left(\mathbf{V}_k^{(i)H}\mathbf{E}_{k',i'}\left(\mathbf{\Lambda}_{k',i'} + \Psi_{k',i'}\cdot d/P\,\mathbf{I}\right)\mathbf{E}_{k',i'}^H\mathbf{V}_k^{(i)}\right)} \qquad ,(3.24) \\
\Leftrightarrow &\max_{\mathbf{V}_k^{(i)}} \frac{\mathbf{V}_k^{(i)H}\mathbf{H}_k^H\mathbf{U}^{((k-1)d+i)}\mathbf{U}^{((k-1)d+i)H}\mathbf{H}_k\mathbf{V}_k^{(i)}}{\prod_{\substack{k',i' \\ (k',i')\neq(k,i)}} \left(\mathbf{V}_k^{(i)H}\mathbf{E}_{k',i'}\mathbf{\Lambda}'_{k',i'}\mathbf{E}_{k',i'}^H\mathbf{V}_k^{(i)}\right)}
\end{aligned}$$

where $\mathbf{\Lambda}'_{k',i'} = \mathbf{\Lambda}_{k',i'} + \frac{\Psi_{k',i'}d}{P}\mathbf{I} = diag\begin{bmatrix}\alpha_{k',i'} + \frac{\Psi_{k',i'}d}{P} & \frac{\Psi_{k',i'}d}{P} & \cdots & \frac{\Psi_{k',i'}d}{P}\end{bmatrix}$. Let $\mathbf{\Lambda}''_{k',i'} = \frac{\mathbf{\Lambda}'_{k',i'}}{\Psi_{k',i'}d/P} = diag\begin{bmatrix}\frac{\alpha_{k',i'}P/d + \Psi_{k',i'}}{\Psi_{k',i'}} & 1 & \cdots & 1\end{bmatrix} = diag\begin{bmatrix}\lambda_{k',i'} & 1 & \cdots & 1\end{bmatrix}$, (3.24) can be reformulated as:

$$\begin{aligned}
&\max_{\mathbf{V}_k^{(i)}} \frac{\mathbf{V}_k^{(i)H}\mathbf{H}_k^H\mathbf{U}^{((k-1)d+i)}\mathbf{U}^{((k-1)d+i)H}\mathbf{H}_k\mathbf{V}_k^{(i)}}{\prod_{\substack{k',i' \\ (k',i')\neq(k,i)}} \left(\mathbf{V}_k^{(i)H}\mathbf{E}_{k',i'}\left(\Psi_{k',i'}d/P\,\mathbf{\Lambda}''_{k',i'}\right)\mathbf{E}_{k',i'}^H\mathbf{V}_k^{(i)}\right)} \\
\Leftrightarrow &\max_{\mathbf{V}_k^{(i)}} \frac{\mathbf{V}_k^{(i)H}\mathbf{H}_k^H\mathbf{U}^{((k-1)d+i)}\mathbf{U}^{((k-1)d+i)H}\mathbf{H}_k\mathbf{V}_k^{(i)}}{\prod_{\substack{k',i' \\ (k',i')\neq(k,i)}} \Psi_{k',i'}d/P\left(\mathbf{V}_k^{(i)H}\mathbf{E}_{k',i'}\mathbf{\Lambda}''_{k',i'}\mathbf{E}_{k',i'}^H\mathbf{V}_k^{(i)}\right)} \qquad . \qquad (3.25) \\
\Leftrightarrow &\max_{\mathbf{V}_k^{(i)}} \frac{\mathbf{V}_k^{(i)H}\mathbf{H}_k^H\mathbf{U}^{((k-1)d+i)}\mathbf{U}^{((k-1)d+i)H}\mathbf{H}_k\mathbf{V}_k^{(i)}}{\left(\prod_{\substack{k',i' \\ (k',i')\neq(k,i)}} \Psi_{k',i'}d/P\right)\cdot\prod_{\substack{k',i' \\ (k',i')\neq(k,i)}} \left(\mathbf{V}_k^{(i)H}\mathbf{E}_{k',i'}\mathbf{\Lambda}''_{k',i'}\mathbf{E}_{k',i'}^H\mathbf{V}_k^{(i)}\right)}
\end{aligned}$$

The result of (3.25) implies:

$$\max_{\mathbf{V}_k^{(i)}} \frac{\mathbf{V}_k^{(i)H}\mathbf{H}_k^H\mathbf{U}^{((k-1)d+i)}\mathbf{U}^{((k-1)d+i)H}\mathbf{H}_k\mathbf{V}_k^{(i)}}{\prod\limits_{\substack{k',i'\\(k',i')\neq(k,i)}} \mathbf{V}_k^{(i)H}\left(\mathbf{E}_{k',i'}\boldsymbol{\Lambda}''_{k',i'}\mathbf{E}_{k',i'}^H\right)\mathbf{V}_k^{(i)}}$$
$$\Leftrightarrow \max_{\mathbf{V}_k^{(i)}} \frac{\mathbf{V}_k^{(i)H}\mathbf{H}_k^H\mathbf{U}^{((k-1)d+i)}\mathbf{U}^{((k-1)d+i)H}\mathbf{H}_k\mathbf{V}_k^{(i)}}{\prod\limits_{\substack{k',i'\\(k',i')\neq(k,i)}} \mathbf{V}_k^{(i)H}\left(\lambda_{k',i'}\mathbf{E}_{k',i'}^{(1)}\mathbf{E}_{k',i'}^{(1)H}+\sum_{t\neq 1}\mathbf{E}_{k',i'}^{(t)}\mathbf{E}_{k',i'}^{(t)H}\right)\mathbf{V}_k^{(i)}} . \quad (3.26)$$

If $\lambda_{k'\max,i'\max}$ is maximum among $\left\{\lambda_{k',i'}, k'\in\{1,\cdots K\}, i'\in\{1,\cdots d\}, (k',i')\neq(k,i)\right\}$, (3.26) can be shown as

$$\max_{\mathbf{V}_k^{(i)}} \frac{\mathbf{V}_k^{(i)H}\mathbf{H}_k^H\mathbf{U}^{((k-1)d+i)}\mathbf{U}^{((k-1)d+i)H}\mathbf{H}_k\mathbf{V}_k^{(i)}}{\mathbf{V}_k^{(i)H}\left(\lambda_{k'\max,i'\max}\mathbf{E}_{k'\max,i'\max}^{(1)}\mathbf{E}_{k'\max,i'\max}^{(1)H}+\sum_{t\neq 1}\mathbf{E}_{k'\max,i'\max}^{(t)}\mathbf{E}_{k'\max,i'\max}^{(t)H}\right)\mathbf{V}_k^{(i)}\cdot\kappa} \quad (3.27)$$

$$\kappa=\frac{\prod\limits_{\substack{k',i'\\(k',i')\neq(k,i)}} \mathbf{V}_k^{(i)H}\left(\lambda_{k',i'}\mathbf{E}_{k',i'}^{(1)}\mathbf{E}_{k',i'}^{(1)H}+\sum_{t\neq 1}\mathbf{E}_{k',i'}^{(t)}\mathbf{E}_{k',i'}^{(t)H}\right)\mathbf{V}_k^{(i)}}{\mathbf{V}_k^{(i)H}\left(\lambda_{k'\max,i'\max}\mathbf{E}_{k'\max,i'\max}^{(1)}\mathbf{E}_{k'\max,i'\max}^{(1)H}+\sum_{t\neq 1}\mathbf{E}_{k'\max,i'\max}^{(t)}\mathbf{E}_{k'\max,i'\max}^{(t)H}\right)\mathbf{V}_k^{(i)}} . \quad (3.28)$$

Based on the discussion above, we can approximate (3.27) as

$$\max_{\mathbf{V}_k^{(i)}} \frac{\mathbf{V}_k^{(i)H}\mathbf{H}_k^H\mathbf{U}^{((k-1)d+i)}\mathbf{U}^{((k-1)d+i)H}\mathbf{H}_k\mathbf{V}_k^{(i)}}{\mathbf{V}_k^{(i)H}\tilde{\mathbf{B}}_k^{(i)}\mathbf{V}_k^{(i)}}, \quad (3.29)$$

$$\begin{aligned}\tilde{\mathbf{B}}_k^{(i)} &= \mathbf{E}_{k'\max,i'\max}\boldsymbol{\Lambda}''_{k'\max,i'\max}\mathbf{E}_{k'\max,i'\max}^H \\ &= \lambda_{k'\max,i'\max}\mathbf{E}_{k'\max,i'\max}^{(1)}\mathbf{E}_{k'\max,i'\max}^{(1)H}+\sum_{t\neq 1}\mathbf{E}_{k'\max,i'\max}^{(t)}\mathbf{E}_{k'\max,i'\max}^{(t)H}\end{aligned}, \quad (3.30)$$

which yields:

$$\mathbf{V}_k^{(i)}=\mu_k\frac{\left(\tilde{\mathbf{B}}_k^{(i)}\right)^{-1}\mathbf{H}_k^H\mathbf{U}^{((k-1)d+i)}}{\left\|\left(\tilde{\mathbf{B}}_k^{(i)}\right)^{-1}\mathbf{H}_k^H\mathbf{U}^{((k-1)d+i)}\right\|}, \quad (3.31)$$

$\forall i\in\{1,2,\cdots,d\}, \forall k\in\{1,2,\cdots,K\}$. μ_k is chosen to satisfy $\mathrm{tr}(\mathbf{V}_k\mathbf{V}_k^H)=P$. The detail of the iterative procedure for our proposed IA aided UL CoMP transceiver design is

summarized in **Table 3-2**.

Table 3-2: Iterative procedure for the proposed IA aided UL CoMP transceiver design

Step 1.	Start with arbitrary precoders $\mathbf{V}_k$, $\forall k \in \{1, 2, \ldots, K\}$
Step 2.	Compute the joint decoder **U** column by column using (3.18) to achieve better SINR performance with $\mathbf{V}_k$ obtained from previous step, $\forall k \in \{1, 2, \ldots, K\}$.
Step 3.	Compute precoder $\mathbf{V}_k$ column by column by equation (3.31) to achieve better SINR performance with **U** obtained from previous step, $\forall k \in \{1, 2, \ldots, \mathrm{K}\}$.
Step 4.	Go back to **Step 2** unless the number of iterations reaches a predefined limit.

3.4 Computer Simulations

The convergence behavior and sum-rate performance evaluations are presented for comparison between the UL CoMP transceiver scheme assisted with Min Leakage-IA, the UL CoMP transceiver scheme assisted with Max SINR-IA, and the proposed IA aided UL CoMP transceiver design which are called "Min Leakage-UL CoMP", "Max SINR-UL CoMP", and "IA aided UL CoMP", respectively. The achievable sum-rate is calculated based on (2.7) mentioned in chapter 2 because a linear MMSE receiver is adopted in our work. $\tilde{\gamma}_k^i$ involved in (2.7) is illustrated in **Figure 3-2**. Furthermore, sum capacity of UL CoMP with full BS cooperation also exhibits as a performance upper bound [15]. The simulation parameters chosen in this section are listed in **Table 3-3**.

Table 3-3: Simulation parameters

Parameter	Value
Channel	i.i.d. Rayleigh fading channel
Number of BSs / UEs (K)	3
Number of transmit antennas (M_t)	4
Number of receive antennas (M_r)	2, 4
Number of transmitted signal layers (d)	2, 3
Number of channel realizations	100 (sum-rate performance) 5000 (convergence behavior)
Number of iterations for each algorithm	20 (sum-rate performance)

The convergence behavior are provided in **Figure 3-4** and **Figure 3-5** both of which are evaluated at SNR = 10 dB and at SNR = 30 dB. **Figure 3-4** is simulated in the case with M_t=4, M_r=2, K=3, d=2; **Figure 3-5** is simulated in the case with M_t=4, M_r=4, K=3, d=3. The simulation results show that Min Leakage-UL CoMP, Max SINR-UL CoMP, and IA aided UL CoMP have superior convergence behavior in all cases especially for Min Leakage-UL CoMP. However, large rate degradation occurs when Min Leakage-UL CoMP is adopted which is consisted with the numerical evaluation in section 3.2. This is because Min Leakage-UL CoMP mechanism makes all its effort to minimize the interference leakage but assumes (3.2) is automatically satisfied; hence there is no assurance that the received power of desired signal can achieve an acceptable level as mentioned in section 3.2.

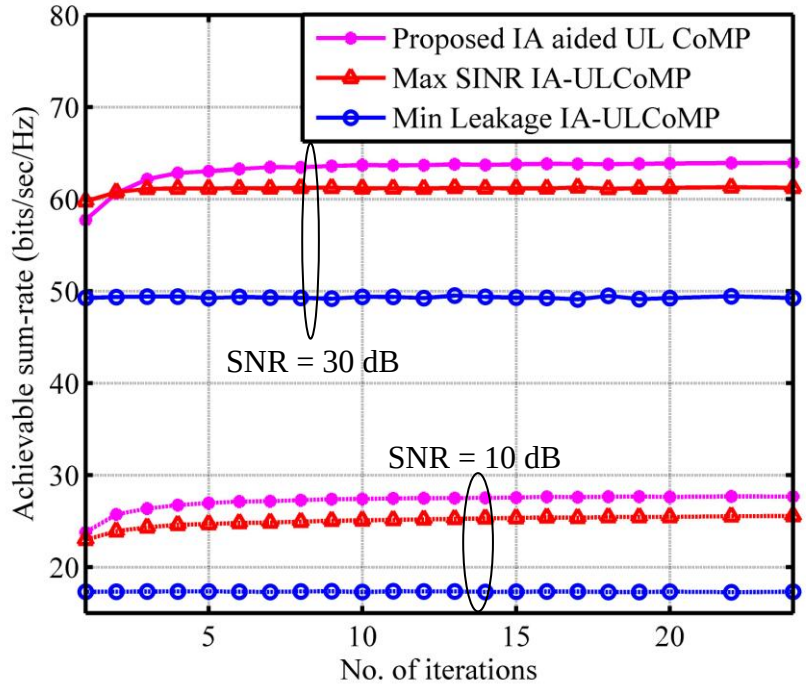

Figure 3-4: Rate convergence behavior of Min Leakage-UL CoMP, Max SINR-UL CoMP, and IA aided UL CoMP with M_t=4, M_r=2, K=3, d=2, and SNR = 10/30 (dB)

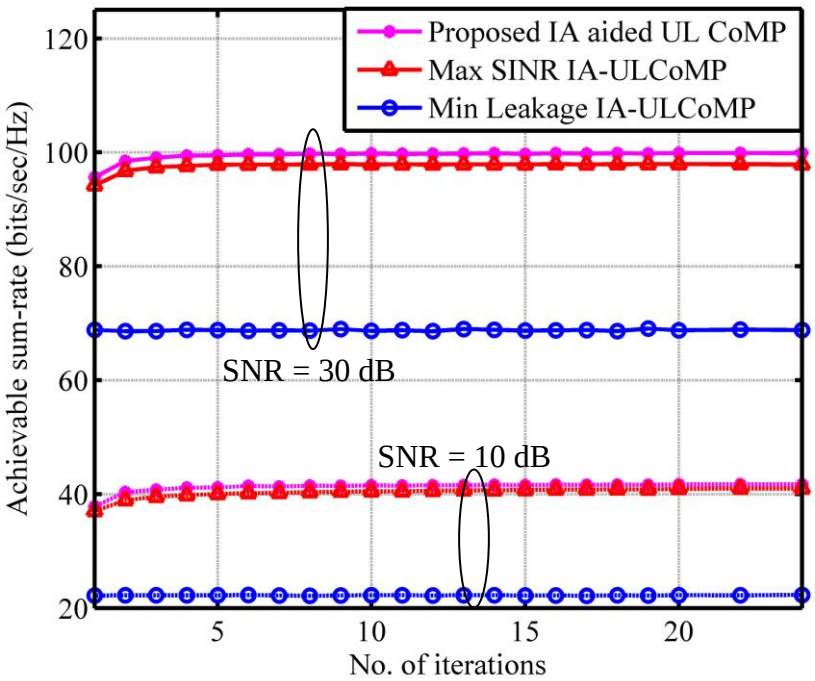

Figure 3-5: Rate convergence behavior of Min Leakage-UL CoMP, Max SINR-UL CoMP, and IA aided UL CoMP with M_t=4, M_r=4, K=3, d=3, and SNR = 10/30 (dB)

In **Figure 3-6** and **Figure 3-7**, sum-rate performance comparisons between Min Leakage-UL CoMP, Max SINR-UL CoMP, and IA aided UL CoMP are displayed. **Figure 3-6** is simulated in the case with M_t=4, M_r=2, K=3, d=2; **Figure 3-7** is simulated in the case with M_t=4, M_r=4, K=3, d=3. In all cases, it is found that Min Leakage-UL CoMP has substantial rate degradation compared to other two UL CoMP transceiver schemes due to its poor ability to maintain the received power of desired signal as mentioned above. The simulations also show that Max SINR-UL CoMP can achieve acceptable sum-rate performance as expected, and the proposed IA aided UL CoMP can reach even better sum-rate performance than Max SINR-UL CoMP. This is because that the proposed IA aided UL CoMP has the effect of balancing the SINR of each layer at the decoder output to improve the condition of the effective channel matrix. The sum capacity is provided here as a performance upper bound. We can find that the achievable sum-rate of IA aided UL CoMP is sufficiently close to the sum capacity especially for the case with M_t=4, M_r=2, K=3, d=2.

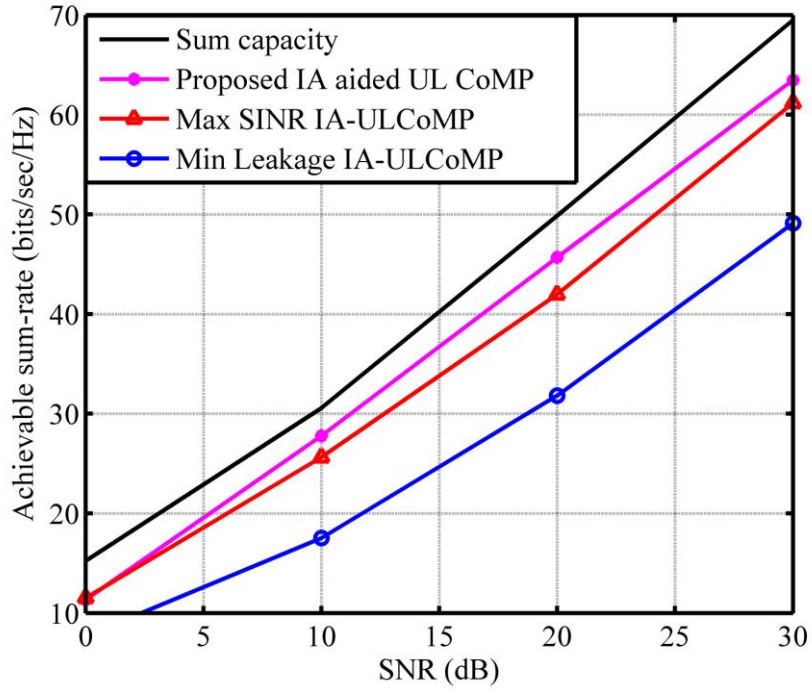

Figure 3-6: Sum-rate performance of Min Leakage-UL CoMP, Max SINR-UL CoMP, and IA aided UL CoMP with M_t=4, M_r=2, K=3, and d=2

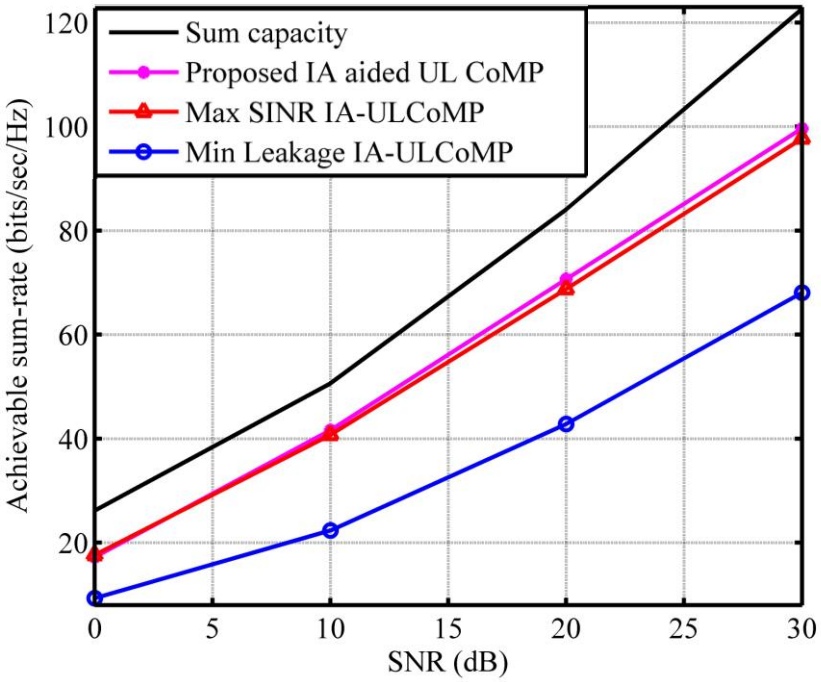

Figure 3-7: Sum-rate performance of Min Leakage-UL CoMP, Max SINR-UL CoMP, and IA aided UL CoMP with M_t=4, M_r=4, K=3, and d=3

3.5 Summary

Interference alignment assisted UL CoMP is discussed and evaluated comprehensively in this chapter. First, two popular interference alignment algorithms, Min Leakage-IA and Max SINR-IA [9], [12], developed in *K*-user interference channel are incorporated in the UL CoMP transceiver designs which are called Min Leakage-UL CoMP and Max SINR-UL CoMP, respectively. Their sum-rate performance are evaluated and it is demonstrated that Max SINR-UL CoMP has better sum-rate performance since a good compromise between interference and received power of desired signal can be preserved. Hence Max SINR-UL CoMP is regarded as a highly potential interference mitigation scheme. According to the study in the first stage, an IA aided UL CoMP transceiver scheme that incorporates the basic idea of Max SINR-UL CoMP and further balances the SINR of each layer at the output of decoder is proposed. The simulation results show that the proposed IA-aided UL CoMP transceiver can achieve superior sum-rate and convergence performance.

Chapter 4

Channel Condition Enhanced Transceiver Design

In the thesis, two centralized UL CoMP transceiver schemes are introduced and both of which are established based on the joint processing nature provided by full BS cooperation. One of the UL CoMP transceiver schemes aided by IA is presented in Chapter 3. The other one aiming at enhancing the condition of the effective channel is given in this chapter.

The proposed channel condition enhanced UL CoMP transceiver scheme involves an iterative procedure which is similar to the iterative procedure included in IA aided UL CoMP transceiver design mentioned in Chapter 3, and each iteration consists of two stages: 1) to calculate the joint decoder and 2) to compute the precoders. But unlike IA aided UL CoMP transceiver, the precoders in the channel condition enhanced scheme is obtained by exploiting the UL-DL duality where the centralized UL CoMP (MAC-like structure) is dual to the virtual centralized DL CoMP (broadcast channel-like structure, BC-like structure) by reversing the direction of communication.

The arrangement of this thesis is as follows. In section 4.1, the motivation of the proposed channel condition enhanced UL CoMP transceiver scheme is provided. Then the problem formulation and design procedure of the proposed channel condition

enhanced scheme are described in section 4.2. Next, we analyze the complexity behavior of the two proposed transceiver schemes in section 4.3, which is followed by the numerical simulations including evaluations of convergence behavior, achievable sum-rate performance, sensitivity to the initial value in the iterative procedure, and the fairness between different users in section 4.4. Last of all, we summarize this chapter in section 4.5.

4.1 Motivation

Due to full BS cooperation, a MAC-like structure and an effective channel matrix as shown in (2.5) are formed in centralized UL CoMP. The state of the effective channel matrix is a crucial factor in transceiver design and can significantly affect the system performance; hence we attempt to properly design the precoders and the joint decoder to induce a well-behaved effective channel matrix. In this thesis, two UL CoMP transceiver schemes for creating a well-behaved effective channel are proposed.

In Chapter 3, an IA-aided UL CoMP transceiver is proposed from the viewpoint of interference alignment and interference mitigation. The algorithm tries to reduce the residual interference and to increase the received power of the desired signal for each layer at the output of decoder. Then a near diagonal effective channel matrix is accomplished since the algorithm will somehow enlarge the ratio of diagonal terms to off-diagonal terms. On the other hand, in this chapter, we endeavor to develop a UL CoMP transceiver scheme which tries to enhance the effective channel condition.

It is well known that the effective channel matrix in a good condition must have small condition number and large singular values. Therefore, we try to develop a transceiver design criterion that can minimize the condition number and can maximize the singular values simultaneously. The proposed channel condition enhanced

transceiver is described in section 4.2.

4.2 Proposed Channel Condition Enhanced Transceiver

The proposed channel condition enhanced transceiver provided in this section attempts to properly design the precoders and the joint decoder such that a well-conditioned effective channel can be achieved by minimizing the condition number and maximizing the singular values of the effective channel matrix in the same time. The basic structure of the iteration process is similar to the one adopted in IA aided UL CoMP transceiver in section 3.3, where in each iteration, two stages are involved: 1) to calculate the joint decoder and 2) to compute the precoders. However, in the second stage, the precoders is obtained according to the virtual centralized DL CoMP (BC-like structure) by exploiting the UL-DL duality in the channel condition enhanced transceiver scheme, which is different from the IA aided UL CoMP transceiver.

In the first stage, the joint decoder is calculated. To minimize the condition number and to maximize the singular values of the effective channel matrix, the following two criteria should be achieved:

$$\min_{\mathbf{U}^{((k-1)d+i)}} \mathcal{K}\left(\tilde{\mathbf{H}}\right) = \frac{\sigma_{\max}}{\sigma_{\min}}, \tag{4.1}$$

$$\max_{\mathbf{U}^{((k-1)d+i)}} \sigma_i, \forall i \in \{1, 2, \cdots, d\}, \tag{4.2}$$

where $\mathcal{K}\left(\tilde{\mathbf{H}}\right)$ denotes the condition number of effective channel matrix, $\tilde{\mathbf{H}}$; $\sigma_{\max}$ and $\sigma_{\min}$ stand for the maximum and minimum singular value of $\tilde{\mathbf{H}}$, respectively; the singular value decomposition of $\tilde{\mathbf{H}}$ is given by $\mathbf{A}\sum\mathbf{B}^H$, where

$\Sigma = diag\{\sigma_1 \quad \sigma_2 \quad \ldots \quad \sigma_d\}$ is a diagonal matrix with singular values on the diagonal; $\mathbf{A}$ and $\mathbf{B}$ are unitary matrices, respectively.

To achieve (4.1) and (4.2), the objective function of our proposed algorithm is formulated as follows:

$$\max_{\mathbf{U}^{((k-1)d+i)}} \prod_i \sigma_i , \tag{4.3}$$

which attempts to increase each of the singular value. In the meantime, the difference between the singular values will somehow be reduced due to the operation of product in (4.3). (4.3) can be equally expressed as

$$\max_{\mathbf{U}^{((k-1)d+i)}} \left(\prod_i \sigma_i \right)^2 = \max_{\mathbf{U}^{((k-1)d+i)}} \prod_i (\sigma_i)^2 . \tag{4.4}$$

With the following derivation,

$$\begin{aligned} \tilde{\mathbf{H}}\tilde{\mathbf{H}}^H &= \mathbf{A}\Sigma\mathbf{B}^H\mathbf{B}\Sigma\mathbf{A}^H \\ &= \mathbf{A}\Sigma^2\mathbf{A}^H \\ &= \mathbf{A}\begin{bmatrix} \sigma_1^2 & & & 0 \\ & \sigma_2^2 & & \\ & & \ddots & \\ 0 & & & \sigma_d^2 \end{bmatrix}\mathbf{A}^H \end{aligned} , \tag{4.5}$$

the eigenvalue decomposition of $\tilde{\mathbf{H}}\tilde{\mathbf{H}}^H$ is given and can be shown as follows:

$$\tilde{\mathbf{H}}\tilde{\mathbf{H}}^H = \mathbf{A}\begin{bmatrix} \lambda_1 & & & 0 \\ & \lambda_2 & & \\ & & \ddots & \\ 0 & & & \lambda_{d_k} \end{bmatrix}\mathbf{A}^H \tag{4.6}$$

where $\lambda_i = \sigma_i^2$ depicts the eigenvalue of $\tilde{\mathbf{H}}\tilde{\mathbf{H}}^H$. Hence (4.4) can be expressed as,

$$\max_{\mathbf{U}^{((k-1)d+i)}} \prod_i \lambda_i . \tag{4.7}$$

According to the property that the product of the eigenvalues is equal to the determinant of $\tilde{\mathbf{H}}\tilde{\mathbf{H}}^H$, we can reformulate (4.7) as,

$$\max_{\mathbf{U}^{((k-1)d+i)}} \det\left(\tilde{\mathbf{H}}\tilde{\mathbf{H}}^H\right). \tag{4.8}$$

$\tilde{\mathbf{H}}$ is a square matrix with size $(dK)\times(dK)$, and the fact leads to

$$\max_{\mathbf{U}^{((k-1)d+i)}} \det\left(\tilde{\mathbf{H}}\right)\cdot\det\left(\tilde{\mathbf{H}}^H\right) = \max_{\mathbf{U}^{((k-1)d+i)}} \det\left(\tilde{\mathbf{H}}\right)\cdot\det\left(\tilde{\mathbf{H}}\right)^*, \tag{4.9}$$

which is equal to

$$\max_{\mathbf{U}^{((k-1)d+i)}} \left|\det\left(\tilde{\mathbf{H}}\right)\right|^2. \tag{4.10}$$

Due to $\tilde{\mathbf{H}} = \mathbf{U}^H\mathbf{H}\mathbf{V}$ mentioned in (2.5), (4.10) can be equally expressed as

$$\max_{\mathbf{U}^{((k-1)d+i)}} \left|\det\left(\mathbf{U}^H\mathbf{H}\mathbf{V}\right)\right|^2. \tag{4.11}$$

Based on Laplace expansion by minors along row $(k-1)d+i$, we can obtain,

$$\max_{\mathbf{U}^{((k-1)d+i)}} \left|\mathbf{U}^{((k-1)d+i)H}\mathbf{H}\mathbf{V}\mathbf{a}_{k,i}\right|^2 = \max_{\mathbf{U}^{((k-1)d+i)}} \left|\mathbf{U}^{((k-1)d+i)H}\mathbf{b}_{k,i}\right|^2, \tag{4.12}$$

where $\left[\mathbf{a}_{k,i}^H\right]_{(q)}$ is the cofactor of $\left[\mathbf{U}^{((k-1)d+i)H}\mathbf{H}\mathbf{V}\right]_{(q)}$, $\forall q \in \{1, 2, \cdots, d\cdot K\}$, and $\mathbf{b}_{k,i} = \mathbf{H}\mathbf{V}\mathbf{a}_{k,i}$. Then according to Cauchy–Schwarz inequality, we can obtain the following inequality,

$$\left|\mathbf{U}^{((k-1)d+i)H}\mathbf{b}_{k,i}\right|^2 \le \left(\mathbf{U}^{((k-1)d+i)H}\mathbf{U}^{((k-1)d+i)}\right)\left(\mathbf{b}_{k,i}^H\mathbf{b}_{k,i}\right). \tag{4.13}$$

With the assumption, $\mathbf{U}^{((k-1)d+i)H}\mathbf{U}^{((k-1)d+i)} = \left\|\mathbf{U}^{((k-1)d+i)}\right\|^2 = 1$, (4.13) is equal to

$$\left|\mathbf{U}^{((k-1)d+i)H}\mathbf{b}_{k,i}\right|^2 \le \left(\mathbf{b}_{k,i}^H\mathbf{b}_{k,i}\right) = \left\|\mathbf{b}_{k,i}\right\|^2. \tag{4.14}$$

Based on (4.12) and the inequality in (4.14), the joint decoder can be obtained:

$$\mathbf{U}^{((k-1)d+i)} = \frac{\mathbf{b}_{k,i}}{\left\|\mathbf{b}_{k,i}\right\|} = \frac{\mathbf{H}\mathbf{V}\mathbf{a}_{k,i}}{\left\|\mathbf{H}\mathbf{V}\mathbf{a}_{k,i}\right\|}, \tag{4.15}$$

$\forall i \in \{1,2,\cdots,d\}, \forall k \in \{1,2,\cdots,K\}$.

In the second stage, the precoders are computed based on the virtual DL CoMP system by exploiting the UL-DL duality, where the effective channel matrix can be expressed as

$$\bar{\mathbf{H}} = \mathbf{V}^H \mathbf{H}^H \mathbf{U}. \tag{4.16}$$

Following the same derivation in the joint decoder design, we can obtain the objective function shown below:

$$\max_{\mathbf{V}_k^{(i)}} \left|\det\left(\bar{\mathbf{H}}\right)\right|^2 = \max_{\mathbf{V}_k^{(i)}} \left|\det\left(\mathbf{V}^H \mathbf{H}^H \mathbf{U}\right)\right|^2, \tag{4.17}$$

Similar to (4.12), we can calculate the determinant based on Laplace expansion by minors along row $(k-1)d+i$,

$$\max_{\mathbf{V}_k^{(i)}} \left|\mathbf{V}_k^{(i)H} \mathbf{H}_k^H \mathbf{U}\tilde{\mathbf{a}}_{k,i}\right|^2 = \max_{\mathbf{V}_k^{(i)}} \left|\mathbf{V}_k^{(i)H} \tilde{\mathbf{b}}_{k,i}\right|^2 \tag{4.18}$$

where $\left[\tilde{\mathbf{a}}_{k,i}^H\right]_{(q)}$ is the cofactor of $\left[\mathbf{V}_k^{(i)H} \mathbf{H}_k^H \mathbf{U}\right]_{(q)}$, $\forall q$, and $\tilde{\mathbf{b}}_{k,i} = \mathbf{H}_k^H \mathbf{U}\tilde{\mathbf{a}}_{k,i}$. According to Cauchy–Schwarz inequality and with the following assumption,

$$\mathbf{V}_k^{(i)H} \mathbf{V}_k^{(i)} = \left\|\mathbf{V}_k^{(i)}\right\|^2 = 1, \tag{4.19}$$

we can obtain the precoders:

$$\mathbf{V}_k^{(i)} = \mu_k \frac{\mathbf{H}_k^H \mathbf{U}\tilde{\mathbf{a}}_{k,i}}{\left\|\mathbf{H}_k^H \mathbf{U}\tilde{\mathbf{a}}_{k,i}\right\|}, \tag{4.20}$$

where μ_k is chosen to satisfy $\mathrm{tr}(\mathbf{V}_k \mathbf{V}_k^H) = P$. The detail of the iteration procedure is listed in **Table 4-1**.

Table 4-1: Iterative procedure for the proposed channel condition enhanced transceiver

Step 1.	Start with arbitrary precoders $\mathbf{V}_k$, $\forall k \in \{1, 2, \ldots, K\}$
Step 2.	Compute the joint decoder **U** column by column using (4.15) to achieve better effective channel condition with $\mathbf{V}_k$ obtained from previous step, $\forall k \in \{1, 2, \ldots, K\}$.
Step 3.	Compute precoder $\mathbf{V}_k$ column by column by equation (4.20) based on the virtual DL CoMP system to achieve better effective channel condition with **U** obtained from previous step, $\forall k \in \{1, 2, \ldots, K\}$.
Step 4.	Go back to **Step 2** unless the number of iterations reaches a predefined limit.

4.3 Complexity Analysis of Proposed UL CoMP Transceivers

Computational complexity is a critical issue from the practical viewpoint, and it highly depends on the system parameters and the algorithms adopted. In this section, we give the complexity comparison between the proposed IA aided UL CoMP transceiver mentioned in section 3.3, the proposed channel condition enhanced transceiver mentioned in section 4.2, and the minimum sum mean square error (MSE) transceiver developed in [10], which are called "IA aided UL CoMP", "Channel condition enhanced UL CoMP", and "MMSE UL CoMP", respectively.

Minimum MSE method is a typical approach in transceiver design. Similar to our proposed methods, the transceiver of MMSE UL CoMP is also calculated based on an iterative process, and UL-DL duality is adopted in the precoders design as well. However, the criterion attempts to minimize the sum MSE at the output of the receiver which is different to our designs.

The major computation cost in IA aided UL CoMP involves matrix multiplication, matrix inversion, eigenvalue decomposition, and sort of sequence. In Channel condition enhanced UL CoMP, matrix multiplication, matrix inversion, and computation of determinant are needed. However, for MMSE UL CoMP, only matrix multiplication and matrix inversion are the most computation-consuming operation. The comparison of complexity is summarized in **Table 4-2**, in which the complexity of each algorithm is calculated for each iteration.

Table 4-2: Complexity comparison between different UL CoMP transceiver schemes

Different UL CoMP transceiver schemes	**Complexity per iteration**
I. IA-aided UL CoMP	$\mathcal{O}\begin{pmatrix} K^5 d^2 M_r M_t & d + M_r \\ +K^2 d M_t^2 & M_t d + M_r \end{pmatrix} + K^4 d M_r^3$
II. Channel condition enhanced UL CoMP	$\mathcal{O}\ K^5 d^5 + K^4 d^2 M_r M_t$
III. MMSE UL CoMP [10]	$\mathcal{O}\begin{pmatrix} K^4 M_r & M_t d + M_r M_t + M_r^2 \\ +K M_t^2 & K M_r + M_t \end{pmatrix}$
Comparison	I ≈ II > III

Table 4-2 demonstrates that the proposed IA-aided UL CoMP and Channel condition enhanced UL CoMP achieve comparable computational complexity. The result also shows that MMSE UL CoMP leads to a lower computational complexity compared with the two proposed methods. However, the comparison is based on computation cost per iteration. The simulations in the next section (section 4.4) will show that both of the proposed methods achieve better convergence performance

compared to MMSE UL CoMP, although more calculations are needed per iteration. **Table 4-2** also reveals that more transmit antennas (M_t), receiver antennas (M_r), transmit layers (d), and number of elements in a cooperation group (K) will induce larger complexity per iteration for all cases.

4.4 Computer Simulations

In this section, the numerical evaluations of the proposed iterative "IA aided UL CoMP", the proposed iterative "Channel condition enhanced UL CoMP", and iterative "MMSE UL CoMP" mentioned in [10] are provided. All of the following properties will be numerically simulated: convergence behavior, achievable sum-rate performance, sensitivity to the initial value in the iterative procedure, and the fairness between different users. For all cases, the achievable sum-rate is calculated based on the equation (2.7) mentioned in section 2.2. The simulation parameters chosen in this section are listed in **Table 4-3**.

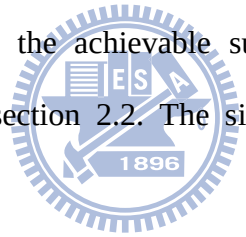

Table 4-3: Simulation parameters

Parameter	**Value**
Channel	i.i.d. Rayleigh fading channel
Number of BSs / UEs (K)	3
Number of transmit antennas (M_t)	4
Number of receive antennas (M_r)	2, 4
Number of transmitted signal layers (d)	2, 3
Number of iterations for each algorithm	10 (except for convergence behavior)

The convergence behaviors are provided in **Figure 4-1** and **Figure 4-2**, both of which are evaluated at SNR = 20 dB and at SNR = 30 dB, and are obtained by averaging over 1000 independent channel realizations. **Figure 4-1** is simulated in the case with M_t=4, M_r=2, K=3, d=2; **Figure 4-2** is simulated in the case with M_t=4, M_r=4, K=3, d=3. The simulation results demonstrate that the proposed Channel condition enhanced UL CoMP can achieve better convergence performance than the proposed IA aided UL CoMP, and the two proposed methods significantly outperform MMSE UL CoMP especially in the high SNR regime. This is because that the co-work of decoder and precoders facilitates the formation of a well-conditioned effective channel matrix. This can improve the condition of effective channel within a few iterations and yield a more efficient iterative processing. **Figure 4-1** and **Figure 4-2** also reveals that although Channel condition enhanced UL CoMP has superior convergence performance, its sum-rate after convergence is a little poorer than the other two methods. This is because that Channel condition enhanced UL CoMP puts all its efforts on effective channel condition enhancing but ignores the effective noise term $\tilde{\mathbf{n}}$ in (2.3), where $\tilde{\mathbf{n}} = \mathbf{U}^H\mathbf{n}$ is a function of the joint decoder. On the other hand, IA aided UL CoMP and MMSE UL CoMP take both interference and noise terms into account and hence can attain better sum-rate after convergence.

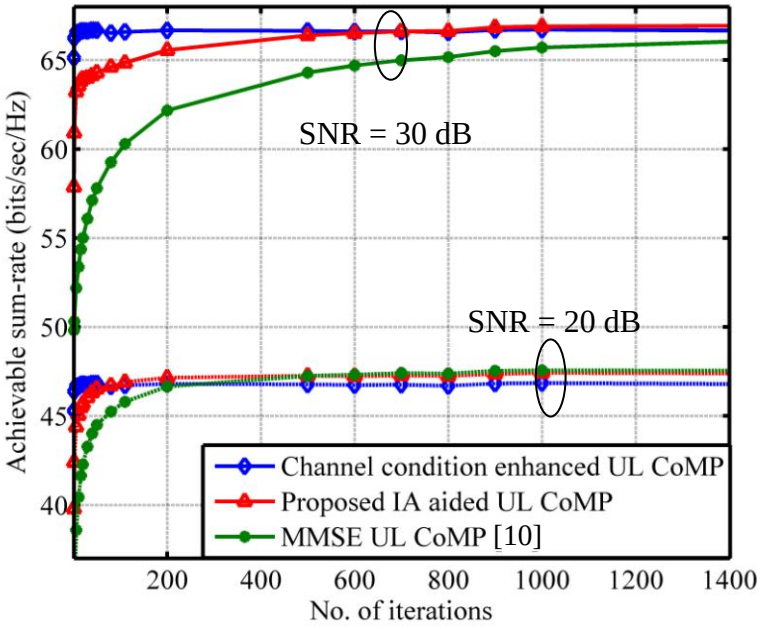

Figure 4-1: Rate convergence behavior of IA aided UL CoMP, Channel condition enhanced UL CoMP, and MMSE UL CoMP with M_t=4, M_r=2, K=3, d=2, and SNR = 20/30 (dB)

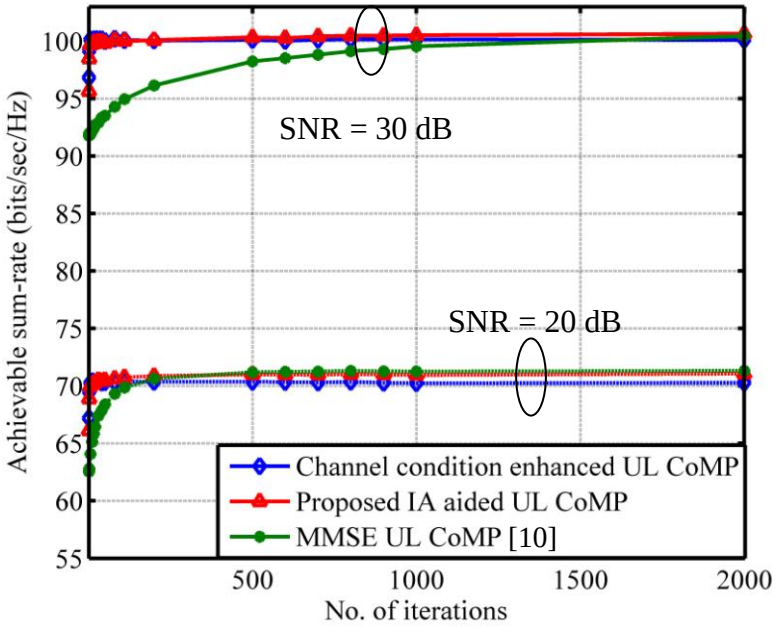

Figure 4-2: Rate convergence behavior of IA aided UL CoMP, Channel condition enhanced UL CoMP, and MMSE UL CoMP with M_t=4, M_r=4, K=3, d=3, and SNR = 20/30 (dB)

In **Figure 4-3** and **Figure 4-4**, sum-rate performance comparisons between IA aided UL CoMP, Channel condition enhanced UL CoMP, and MMSE UL CoMP [10] are displayed. **Figure 4-3** is simulated in the case with M_t=4, M_r=2, K=3, d=2; **Figure 4-4** is simulated in the case with M_t=4, M_r=4, K=3, d=3. In all cases, the simulation results are obtained by averaging over 100 independent channel realizations, and 10 iterations are executed for each iterative algorithm. Sum capacity of UL CoMP with full BS cooperation also exhibits as a performance upper bound [15]. According to the simulation results, we can find that in general Channel condition enhanced UL CoMP achieve better performance than IA aided UL CoMP, and the achievable sum-rate of the proposed two methods are much closer to the sum capacity compared with MMSE UL CoMP especially for the case with M_t=4, M_r=2, K=3, d=2, when 10 iterations are adopted. This is because the two proposed methods both achieve superior convergence performance, that is they can attain pretty good sum-rate performance within few iterations, like 10 iterations, as depicted in **Figure 4-1** and **Figure 4-2**.

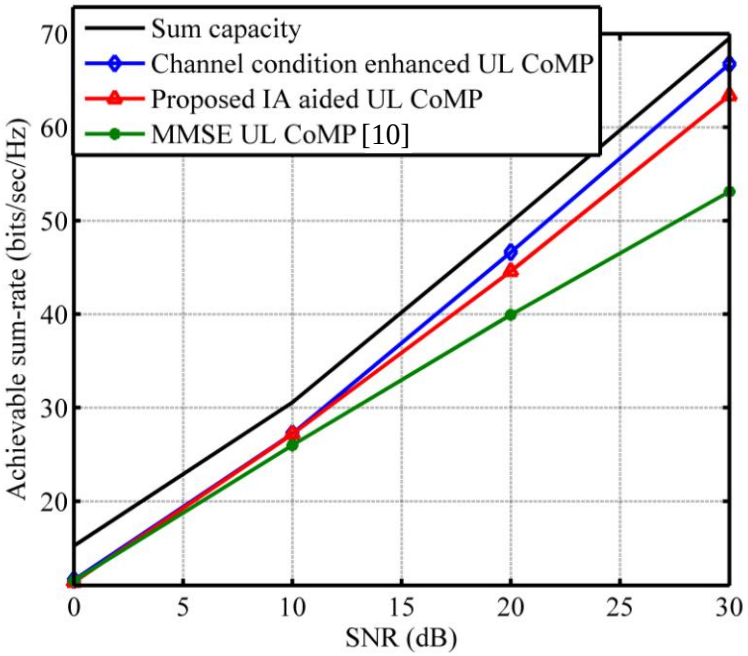

Figure 4-3: Sum-rate performance of IA aided UL CoMP, Channel condition enhanced UL CoMP, and MMSE UL CoMP with M_t=4, M_r=2, K=3, d=2, and no. of iterations=10

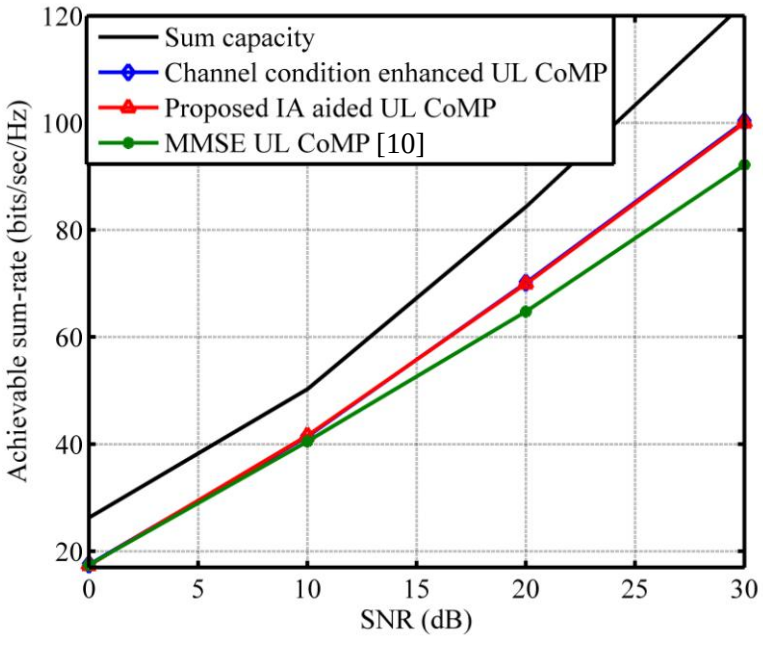

Figure 4-4: Sum-rate performance of IA aided UL CoMP, Channel condition enhanced UL CoMP, and MMSE UL CoMP with M_t=4, M_r=4, K=3, d=3, and no. of iterations=10

In **Figure 4-5**, the comparison of sensitivity to the initial value in the iterative procedure between IA aided UL CoMP, Channel condition enhanced UL CoMP, and MMSE UL CoMP [10] is given. Each algorithm is simulated over 10 iterations under the scenario with M_t=4, M_r=2, K=3, d=2 and is simulated at SNR = 30 dB for a fixed channel realization. The probability density of the sum-rate are calculated based on the output from running different algorithms 100 times, and different initial value ($\mathbf{V}_k$, $\forall k \in \{1, 2, \cdots, K\}$) is adopted each time. In our work, the probability density function is estimated by Parzen window method as the adoption in [14]. The simulation result reveals that the probability density function (pdf) associated with the proposed Channel condition enhanced UL CoMP and IA aided UL CoMP concentrate on the right hand side as shown in **Figure 4-5**, which means that they are more robust to the initial values, and can attain better sum rate performance. On the other hand, the pdf associated with MMSE UL CoMP spreads across a lower-value region. Namely, MMSE UL CoMP is sensitive to the initial values and has worse sum rate performance.

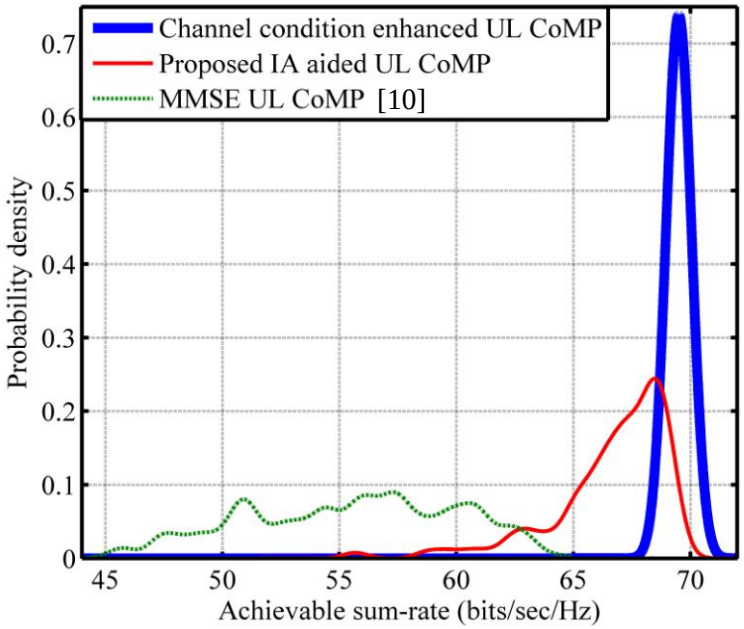

Figure 4-5: Comparison of sensitivity to the initial value in the iterative procedure between IA aided UL CoMP, Channel condition enhanced UL CoMP, and MMSE UL CoMP with M_t=4, M_r=2, K=3, and d=2

In **Figure 4-6**, fairness between different users of IA aided UL CoMP, Channel condition enhanced UL CoMP, and MMSE UL CoMP [10] is provided. Each algorithm is simulated over 10 iterations under the scenario with M_t=4, M_r=2, K=3, d=2 and is simulated at SNR = 30 dB. In all cases, the simulation results are obtained by running 2000 independent channel realizations. The probability density function is also estimated by Parzen window method. In our work, the fairness between different users is defined as follows:

$$\text{Fairness} = \frac{R_{\max} - R_{\min}}{R_{\text{mean}}} \tag{4.21}$$

$$R_{\text{mean}} = \frac{1}{K}\sum_{i=1}^{K} R_i \tag{4.22}$$

where R_i is the achievable sum-rate of ith user. $R_{\max}$ and $R_{\min}$ are the maximum

and minimum values among $\{R_i, i \in \{1, 2, \cdots, K\}\}$, respectively. The simulation demonstrates that the proposed Channel condition enhanced UL CoMP exhibits the best fairness. The proposed IA aided UL CoMP is inferior to Channel condition enhanced UL CoMP. Compared to the proposed two methods, MMSE UL CoMP has the worst property of fairness.

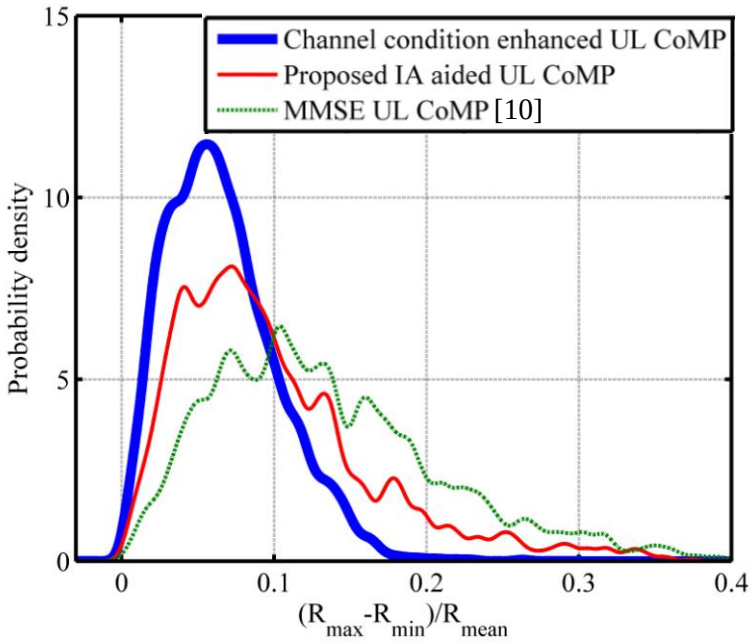

Figure 4-6: Fairness between different users of IA aided UL CoMP, Channel condition enhanced UL CoMP, and MMSE UL CoMP with M_t=4, M_r=2, K=3, and d=2

4.5 Summary

In this chapter, an UL CoMP transceiver scheme based on effective channel condition enhancing is proposed. The proposed Channel condition enhanced UL CoMP attempts to minimize the condition number and to maximize the singular values of the effective channel matrix by maximizing the product of singular values of the effective channel matrix. Next, the comparison of complexity between the proposed IA aided UL

CoMP, the proposed Channel condition enhanced UL CoMP, and MMSE UL CoMP [10] is given, followed by the numerical evaluations of the two proposed methods and MMSE UL CoMP. The results show that the proposed IA aided UL CoMP and the proposed Channel condition enhanced UL CoMP have superior convergence behavior because the co-work of decoder and precoders facilitates the formation of a well-conditioned effective channel matrix, while more computation is needed for each iteration. The simulation results also show that the two proposed methods can achieve rather good sum-rate performance, provide robustness to the initial values in the iterative procedures, and lead to much fairer results, within few iterations, like 10 iterations.

Chapter 5

Conclusions and Future Works

To fulfill the increasing demands and to conduct effective communication in the next generation wireless systems, unity frequency reuses and multiuser transition scheme are adopted, which leads to an interference limited environment. Under such strict environments, coordinated multipoint (CoMP) transmission and reception and multiple input multiple output (MIMO) systems are developed and proposed as two key techniques to achieve advanced performance requirements. In this thesis, we consider uplink CoMP (UL CoMP) assisted with multiple antennas as our system model. According to the potential for system performance improvement, we focus on the case called centralized UL CoMP which can provide full information exchange between BSs and support joint processing at CU. Based on this structure, two associated transceiver schemes are proposed to achieve improved system performance.

Our fist proposed centralized UL CoMP transceiver is developed in Chapter 3 through introducing the idea of interference alignment (IA), a recently emerged interference mitigation technique. The algorithm includes precoders at UEs and a joint decoder at CU followed by the processing of a linear MMSE receiver, and is iterative in nature. Two popular iterative IA algorithms for *K*-user interference channels, Min Leakage-IA and Max SINR-IA [9], [12], are adopted as the candidates in our UL CoMP transceiver design. The UL CoMP transceiver schemes which incorporate Min

Leakage-IA and Max SINR-IA are called Min Leakage-UL CoMP and Max SINR-UL CoMP, respectively. The preliminary evaluation demonstrate that Max SINR-UL CoMP preserves a good compromise between interference and received power of desired signal and can attain better sum-rate performance. Thus, we propose a transceiver scheme, called "IA aided UL CoMP", which can benefit from Max SINR-IA and reach a good balance between the SINRs at the decoder output to maintain the desired system performance.

In Chapter 4, our second proposed centralized UL CoMP transceiver, called "Channel condition enhanced UL CoMP", is introduced. As the transceiver design in IA aided UL CoMP, the second proposed method also includes an iterative algorithm in which precdoers in UEs and a joint decoder at CU are involved. A linear MMSE receiver is employed as well. The basic concept of Channel condition enhanced UL CoMP is to convert the original channel into a more tractable effective channel by enhancing the effective channel condition. It is well known that the effective channel matrix in a good condition must have small condition number and large singular values. Therefore, we develop an algorithm that attempts to minimize the condition number and maximize the singular values of the effective channel matrix at the same time by maximizing the product of singular values iteratively. In the second proposed method, UL-DL duality is also exploited as a key property.

The analysis of complexity shows that more computations are needed per iteration in our two proposed methods compared with MMSE UL CoMP [10]. However, the numerical simulations demonstrate that the proposed IA aided UL CoMP and the proposed Channel condition enhanced UL CoMP substantially outperform MMSE UL CoMP in convergence performance, because the co-work of decoder and precoders facilitates the formation of a well-conditioned effective channel matrix. In addition to the findings above, the simulation results also confirm that compared with MMSE UL

CoMP, the proposed two methods can achieve superior sum-rate performance, provide robustness to the initial values in the iterative procedures, and lead to much fairer results, within few iterations, like 10 iterations.

In the end of the thesis, some possible research directions related to our work are provided as the potential future works. First, based on the results of the numerical simulations, we can find that the proposed Channel condition enhanced UL CoMP exhibits the best convergence behavior, while achieving the worse sum-rate performance after convergence compared to the proposed IA aided UL CoMP. Hence, an Adaptive UL CoMP scheme can be constructed by combining the two proposed methods to attain a superior converge behavior and sum-rate performance at the same time. The idea can be verified by the preliminary evaluations provided in **Figure 5-1** and **Figure 5-2** in which the proposed Channel condition enhanced UL CoMP is executed when the number of iterations is less than 20 to accelerate the rate of convergence, then the proposed IA aided UL CoMP is adopted to achieve better sum-rate performance. So we believe a further advantage can be achieved by combining the proposed Channel condition enhanced UL CoMP and the proposed IA aided UL CoMP. Besides, a robust UL CoMP transceiver design considering channel estimation error is of interest in practical cellular systems because the impact of channel estimation error is inevitable. Next, the issue of power allocation has not been addressed in our work. If we want to further improve the sum-rate performance of the system, a transceiver design incorporating a proper power allocation should be considered. Another issue worth attention is weighted sum-rate maximization which introduces priority between users. Last but not least, to conduct efficient communication in response to channel variation, UL CoMP transceiver design incorporating a mechanism to choose a proper number of transmit layers is desired.

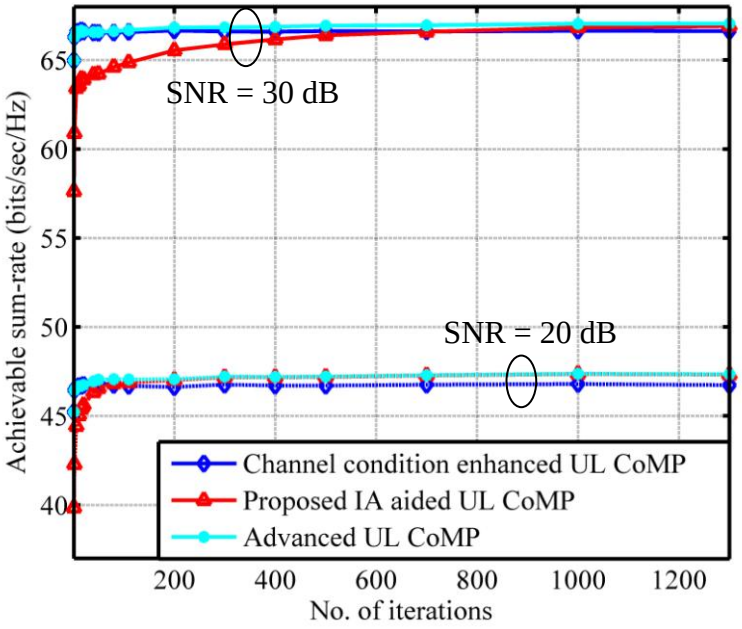

Figure 5-1: Rate convergence behavior of IA aided UL CoMP, Channel condition enhanced UL CoMP, and Advanced UL CoMP with M_t=4, M_r=2, K=3, d=2, and SNR = 20/30 (dB)

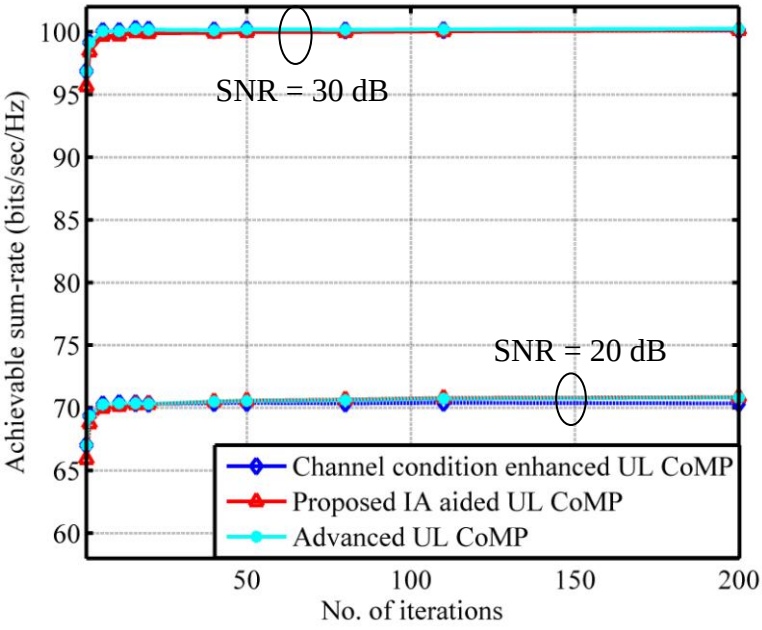

Figure 5-2: Rate convergence behavior of IA aided UL CoMP, Channel condition enhanced UL CoMP, and Advanced UL CoMP with M_t=4, M_r=4, K=3, d=3, and SNR = 20/30 (dB)

Bibliography

[1] 3GPP TR36.819, "Coordinated multi-point operation for LTE physical layer aspects," Dec. 2011.

[2] U. Jang, K. Y. Lee, K. Cho, and W. Ryu, "Transmit beamforming based inter-cell interference alignment and user selection with CoMP," in *Proc. VTC Fall*, 2010, pp.1-5.

[3] P. Marsch and G. Fettweis, "Uplink CoMP under a constrained backhaul and imperfect channel knowledge," *IEEE Trans. Wireless Commun.*, vol. 10, no. 6, pp. 1730-1742, June 2011.

[4] D. Jiang, Q. Wang, J. Liu, G. Liu, and C. Cui, "Uplink coordinated multi-point reception for LTE-Advanced systems," in *Proc. IEEE WiCOM*, 2009, pp. 1-4.

[5] M. Sawahashi, Y. Kishiyama, A. Morimoto, D. Nishikawa, and M. Tanno, "Coordinated multipoint transmission/reception techniques for LTE-advanced," *IEEE Wireless Communications*, vol. 17, no. 3, pp. 26-34, June 2010.

[6] J. G. Andrews, W. Choi, and R. W. Heath Jr., "Overcoming interference in spatial multiplexing MIMO cellular networks," *IEEE Wireless Commun. Mag.*, vol. 14, no. 6, pp. 95–104, Dec. 2007.

[7] A. Tölli, M. Codreanu, and M. Juntti, "Linear multiuser MIMO transceiver

design with quality of service and per-antenna power constraints," *IEEE Trans. Signal Process.*, vol. 56, no. 7, pp. 3049-3055, July 2008.

[8] M. Maddah-Ali, A. Motahari, and A. Khandani, "Communication over MIMO X channels: Interference alignment, decomposition, and performance analysis," *IEEE Trans. Inf. Theory*, vol. 54, no. 8, pp. 3457–3470, Aug. 2008.

[9] K. Gomadam, V. R. Cadambe, and S. A. Jafar, "A distributed numerical approach to interference alignment and applications to wireless interference networks," *IEEE Trans. Inf. Theory*, vol. 57, no. 6, pp. 3309–3322, June 2011.

[10] S. Shi, M. Schubert, and H. Boche , " Downlink MMSE transceiver optimization for multiuser MIMO systems: duality and sum-MSE minimization," *IEEE Trans. Signal Process.*, vol. 55, no. 11, pp. 5436-5446, Nov. 2007.

[11] M. R. McKay, I. B. Collings, and A. M. Tulino, "Achievable sum-rate of MIMO MMSE receivers: A general analytic framework," *IEEE Trans. Inf. Theory*, vol. 56, no. 1, pp. 396 –410, Jan. 2010.

[12] K. Gomadam, V. R. Cadambe, and S. A. Jafar, "Approaching the capacity of wireless networks through distributed interference alignment," in *Proc. IEEE GLOBECOM*, 2008, pp. 1-6.

[13] C. Suh and D. Tse, "Interference alignment for cellular networks," in *Proc. 46th Ann. Allerton Conf. Commun.*, 2008, pp. 1037-1044.

[14] I. Santamaria, O. Gonzalez, R.W. Heath, Jr., and S.W. Peters, "Maximum sum-rate interference alignment algorithms for MIMO channels," in *Proc. IEEE GLOBECOM*, 2010, pp. 1-6.

[15] W. Yu, W. Rhee, S. Boyd, and J. M. Cioffi, "Iterative water-filling for Gaussian vector multiple-access channels," *IEEE Trans. Inf. Theory*, vol. 50, no. 1, pp. 145-152, Jan. 2004.